Convergence of Krylov subspace solvers with Schwarz preconditioner for the exterior Maxwell problem

Eric Darrigrand, Nabil Gmati, Rania Rais

Convergence of Krylov subspace solvers with Schwarz preconditioner for the exterior Maxwell problem

Eric Darrigrand [1], Nabil Gmati [2], Rania Rais [2,3]

[1] *Université de Rennes 1, IRMAR, Campus de Beaulieu, 35042 Rennes, France*
[2] *Université de Tunis El Manar, ENIT, LAMSIN, B.P. 37, 1002 Le Belvédère, Tunisia*
[3] *Université de Kairouan, ISSATK, Avenue Beit El Hekma, 3100 Kairouan, Tunisia*

Dedicated to Professor Peter Monk on the occasion of his 60^{th} birthday!

Abstract

The consideration of an integral representation as an exact boundary condition for the finite element resolution of wave propagation problems in exterior domain induces algorithmic difficulties. In this paper, we are interested in the resolution of an exterior Maxwell problem in 3D. As a first step, we focus on the justification of an algorithm described in literature, using an interpretation as a Schwarz method. The study of the convergence indicates that it depends significantly on the thickness of the domain of computation. This analysis suggests the use of the finite element term of Schwarz method as a preconditioner for use of Krylov iterative solvers. An analytical study of the case of a spherical perfect conductor indicates the efficiency of such approach. The consideration of the preconditioner suggested by the Schwarz method leads to a superlinear convergence of the GMRES predicted by the analytical study and verified numerically.

Keywords: finite element method; integral representation; Krylov solver; Schwarz preconditioner; exterior Maxwell problem.

Introduction

We are interested in the resolution of the 3D exterior time-harmonic Maxwell equations. The problem consists in determining the field diffracted by an obstacle. To solve the equations posed in an unbounded domain, we introduce a fictitious boundary with an artificial boundary condition which models the infinity.

Email addresses: eric.darrigrand-lacarrieu@univ-rennes1.fr (Eric Darrigrand [1]), nabil.gmati@enit.rnu.tn (Nabil Gmati [2]), rania.rais@lamsin.rnu.tn (Rania Rais [2,3]).

In the literature, methods based on a local transparent boundary condition are often considered. They consist in an approximation of the Sommerfeld condition. In this context, we can consider a radiation condition at a finite distance ([7]) or the Bayliss-Gunzburger-Turkel-like conditions ([4,1,16,28]). To obtain satisfying results, the artificial boundary should be chosen far from the boundary of the obstacle. Hence, the computational domain becomes large which increases computation and memory cost. An alternative to local transparent boundary conditions is the Perfectly Matched Layer (PML) method. It consists in replacing the artificial boundary by an absorbing layer of finite elements which vanishes the reflection. The method was introduced by Berenger and derived for the absorption of electromagnetic waves in [8].

In our paper, we rather consider an exact condition defined by an integral representation. The chosen strategy is named "coupling of finite elements and integral representation" and is designated by the acronym CEFRI for the French designation "Couplage Eléments Finis et Représentation Intégrale". CEFRI was initiated in [20] for hydrodynamic problems, and was presented and mathematically studied in the context of electromagnetism equations initially in [19]. In [30,3], a careful study of the numerical behavior of the formulation is presented for 2D Helmholtz equation and 3D Maxwell's equations, based on numerous numerical tests. [30] also includes a study of the convergence of the iterative resolution for the 2D Helmholtz equation. Such an exact condition defined by an integral representation has been successfully applied to the context of Ultra-Weak-Variational Formulation, which is an alternative to the finite elements, where the strategy was coupled to a Fast Multipole Method [15].

Like the consideration of a local transparent boundary condition, CEFRI leads to an equivalent problem posed on a reduced bounded domain delimited by the boundary of the scatterer and the artificial boundary, where the artificial boundary condition is expressed thanks to an integral representation of the unknown on this boundary. Even if integral operators are involved, no singularity occurs because the unknown on the artificial boundary is expressed using the unknown on the boundary of the scatterer. With such an approach, no *a priori* condition is required on the distance between the scatterer and the artificial boundary. The main difficulty consists in the elaboration of a numerical scheme for the resolution because of the integral operators which disturb the usual properties of the discrete equations. In [21], Jin and Liu solved the discrete system by a Jacobi method in order to avoid the inversion of the integral operators. The scheme can be interpreted as a Schwarz method with total overlap. This identification has been initially considered for the Poisson and Helmholtz exterior problems in [5,6]. In our paper, the interpretation is extended to the analytical exploration of the rate of convergence of the resolution strategy for Maxwell's equations. The theoretical analysis of the case of a spherical scatterer indicates that the method converges conditionally on the distance between the scatterer and the artificial boundary. Consequently, using the Jacobi scheme by Jin and Liu, the convergence may fail. However, this study of Schwarz method justifies the use of Krylov solvers and the choice of the preconditioner. We then analytically explore, in this paper, the convergence of a preconditioned GMRES for the resolution of the discrete system and prove the superlinear convergence of the method in the case of a spherical configuration. In [22], Jin and Liu also explored the use of a Krylov solver preconditioned by another formulation of the exterior problem to be solved. Their results are quite similar to ours but the preconditioner is different and consists of more components. In order to verify numerically our theoretical statements, we implemented the resolution strategies using the Finite Element library MÉLINA++ ([23]) which does not provide Nédélec elements. For the numerical results, we then considered the regularized Maxwell equations but the mathematical study of convergence of Jin and Liu algorithm is done for both the classical and the regularized Maxwell equations.

In next section, we introduce the physical problem and explain the application of CEFRI. Section 2 is devoted to the Schwarz interpretation of the resolution strategy suggested in [21]. This consideration enables us to estimate, in Section 3, the speed of convergence of the resolution algorithm in the case of a spherical scatterer using Jin and Liu algorithm. Some test-cases illustrate the theoretical estimation. In Section 4, we investigate the convergence of a Krylov method, the GMRES, combined to the preconditioner

suggested by the previous analysis. Last section provides some numerical simulations which illustrate the convergence properties of this preconditioned application of the GMRES to CEFRI.

1. Scattering by a perfect conductor

Let us consider Ω_i a bounded scatterer in $\mathbb{R}^3$ with Lipschitz-continuous boundary Γ and Ω_e its unbounded complementary. We are concerned with the scattering of a time-harmonic electromagnetic wave by the perfect conductor Ω_i. Our purpose is to determine the total field $E = E^s + E^{inc}$ where E^{inc} is the incident wave and E^s is the scattered field. We then consider the following scattering problem with essential boundary condition on Γ and radiation condition at infinity:

$$\begin{cases} \operatorname{curl}\operatorname{curl} E - k_s^2 E = 0 \text{ in } \Omega_e, \\ E \times n_e = 0 \text{ on } \Gamma, \\ \lim\limits_{R\to\infty} \int_{||x||=R} ||\operatorname{curl} E^s \times n_e - ik_s E^s||^2 d\gamma = 0, \end{cases} \tag{1}$$

where k_s is the wavenumber and n_e is the exterior unit normal. In order to use standard Lagrange finite elements for the numerical resolution, we consider an equivalent elliptic problem by adding a regularizing grad-div term in the time-harmonic Maxwell equations, as described and justified in [19]. Problem (1) is then equivalent to the following one:

$$\begin{cases} \operatorname{curl}\operatorname{curl} E - t^{-1}\nabla(\operatorname{div} E) - k_s^2 E = 0 \text{ in } \Omega_e, \\ E \times n_e = 0, t^{-1}\operatorname{div} E = 0 \text{ on } \Gamma, \\ \lim\limits_{R\to\infty} \int_{||x||=R} ||\operatorname{curl} E^s \times n_e - ik_s n_e \times (E^s \times n_e)||^2 d\gamma = 0, \\ \lim\limits_{R\to\infty} \int_{||x||=R} |\sqrt{t^{-1}}\operatorname{div} E^s - ik_s E^s \cdot n_e|^2 d\gamma = 0, \end{cases} \tag{2}$$

where the regularization term $t^{-1}\nabla(\operatorname{div} E)$ allows the use of a Galerkin finite element method (see [19]) and the regularization parameter t^{-1} depends on the permittivity and the permeability of the air. The parameter t is chosen positive. The choice $t = \infty$ corresponds to the initial scattering problem (1). Many different methods have been developed to solve the time-harmonic Maxwell equations in exterior domains. In this paper, we consider the coupling between finite elements and integral representation introduced by Hazard and Lenoir in [19]. The idea consists in defining an exact boundary condition on an artificial boundary Σ surrounding the scatterer. We reduce the initial problem to an equivalent one, defined on a bounded domain Ω delimited by Γ and Σ. The reduced problem can be stated as follows

$$\begin{cases} \operatorname{curl}\operatorname{curl} E - t^{-1}\nabla(\operatorname{div} E) - k_s^2 E = 0 \text{ in } \Omega, \\ E \times n_\gamma = 0, t^{-1}\operatorname{div} E = 0 \text{ on } \Gamma, \\ T_{\nu_1} E = T_{\nu_1}(E^{inc} - \mathcal{I}_\Gamma^t(E)) \text{ on } \Sigma, \\ N_{\nu_2} E = N_{\nu_2}(E^{inc} - \mathcal{I}_\Gamma^t(E)) \text{ on } \Sigma. \end{cases} \tag{3}$$

where n_γ is the exterior unit normal of the domain Ω_i on Γ. The parameters ν_1 and ν_2 are complex numbers with negative imaginary part. The two operators T_{ν_1} and N_{ν_2} are defined by $T_{\nu_1} E = \operatorname{curl} E \times n_\sigma + \nu_1\, n_\sigma \times (E \times n_\sigma)$ and $N_{\nu_2} E = \operatorname{div} E + \nu_2 E \cdot n_\sigma$ with n_σ the exterior unit normal of the domain Ω

on Σ. The condition that involves N_{ν_2} occurs only if $t \neq \infty$. The boundary conditions on Σ are derived from an integral representation satisfied by the scattered field and identified by the following expression [19]: for $x \in \Omega_e$,

$$\begin{aligned}(\mathcal{I}_\Gamma^t E)(x) = & \int_\Gamma \mathcal{G}_t(x,.)(\operatorname{curl} E \times n_\gamma + t^{-1} n_\gamma \operatorname{div} E) d\gamma \\ & - \int_\Gamma \operatorname{curl}_y \mathcal{G}_t(x,.)(E \times n_\gamma) d\gamma - t^{-1} \int_\Gamma \operatorname{div}_y \mathcal{G}_t(x,.)^T (E \cdot n_\gamma) d\gamma.\end{aligned} \tag{4}$$

where $\mathcal{G}_t = G_{k_s} I + \frac{1}{k_s^2} \mathrm{Hess}(G_{k_s} - G_{k_p})$ is the outgoing Green tensor associated with the differential operator $\operatorname{curl}\operatorname{curl} - t^{-1}\nabla(\operatorname{div}) - k_s^2 I$ of the regularized Maxwell equations; I is the identity matrix in $\mathbb{R}^3$; Hess stands for the Hessian operator; $k_p = \sqrt{t} k_s$; and G_k is the fundamental solution of Helmholtz equation. Due to the essential condition on Γ, $E \times n_\gamma = 0$, the second term of the representation (4) vanishes such that:

$$(\mathcal{I}_\Gamma^t E)(x) = \int_\Gamma \mathcal{G}_t(x,.)(\operatorname{curl} E \times n_\gamma + t^{-1} n_\gamma \operatorname{div} E) d\gamma - t^{-1} \int_\Gamma \operatorname{div}_y \mathcal{G}_t(x,.)^T (E \cdot n_\gamma) d\gamma. \tag{5}$$

The equivalence between the problem stated on the reduced domain Ω (3) and the exterior regularized problem (2) is given by the following proposition (see [19]):

Proposition 1.1 *Choose $\nu_1, \nu_2 \in \mathbb{C}$ with negative imaginary part, then the problems (2) and (3) are equivalent: Problem (2) admits at least (respectively, at most) one solution if and only if it is the same for the reduced problem (3). The following links hold:*

- ⋆ *If E is a solution to (2) then the restriction of E on Ω is a solution to (3).*
- ⋆ *If E_Ω is a solution to (3) then the field E defined by*

$$\begin{cases} E = E_\Omega \text{ in } \Omega, \\ E = E^{inc} - \mathcal{I}_\Gamma^t E_\Omega \text{ in } \Omega_e \backslash \Omega. \end{cases}$$

is a solution to (2).

To ensure existence and uniqueness of the solution, we introduce the following spaces: let $H(\operatorname{curl}, \Omega)$ be the space of fields V satisfying $V \in L^2(\Omega)^3$ and $\operatorname{curl} V \in L^2(\Omega)^3$, and $H(\operatorname{div}, \Omega)$ the space of fields V satisfying $V \in L^2(\Omega)^3$ and $\operatorname{div} V \in L^2(\Omega)$. We then introduce $\mathcal{H}_t$ the Hilbert space required by our problem and defined by

$$\mathcal{H}_t = \left\{ E \in H(\operatorname{curl}, \Omega) \,/ \operatorname{div} E \in L^2(\Omega), E \times n_\gamma = 0, E \times n_\sigma \in L^2(\Sigma)^3, t^{-1} E \cdot n_\sigma \in L^2(\Sigma) \right\}, \tag{6}$$

if $t \neq \infty$, and

$$\mathcal{H}_\infty = \left\{ E \in H(\operatorname{curl}, \Omega), \operatorname{div} E = 0 \text{ in } \Omega, E \times n_\gamma = 0, E \times n_\sigma \in L^2(\Sigma)^3 \right\}. \tag{7}$$

The notation $(.,.)_t$ denotes the natural scalar product on $\mathcal{H}_t$:

$$\begin{aligned}(E, E')_t = & \int_\Omega (E \cdot E' + \operatorname{curl} E \cdot \operatorname{curl} E' + |t|^{-1} \operatorname{div} E \operatorname{div} E') d\Omega \\ & + \int_\Sigma ((E \times n_\sigma) \cdot (E' \times n_\sigma) + |t|^{-1} (E \cdot n_\sigma)(E' \cdot n_\sigma)) d\sigma.\end{aligned}$$

If E is in the space $\mathcal{H}_t$, then $\operatorname{curl} E \times n_\gamma + t^{-1} n_\gamma \operatorname{div} E$ is not defined. We therefore need to extend the definition of $\mathcal{I}_\Gamma^t E$ to $\mathcal{H}_t$ by the consideration of the operator $\mathcal{I}_\Gamma^{t,\mathcal{R}} E$ defined by (see [19] for details): for all $x \in \Omega_e$

$$\begin{aligned}(\mathcal{I}_\Gamma^{t,\mathcal{R}} E)(x) \;=\; & -k_s^2 \int_\Omega \mathcal{R}\mathcal{G}_t(x,.) E \, d\Omega + \int_\Omega \operatorname{curl} \mathcal{R}\mathcal{G}_t(x,.) \operatorname{curl} E \, d\Omega \\ & + \; t^{-1} \int_\Omega \operatorname{div} \mathcal{R}\mathcal{G}_t(x,.)^T \operatorname{div} E \, d\Omega - t^{-1} \int_\Gamma \operatorname{div} \mathcal{G}_t(x,.)^T (E \cdot n_\gamma) d\gamma \,,\end{aligned} \tag{8}$$

where $\mathcal{R}$ is a linear operator that maps every smooth function φ defined on Γ into a smooth function $\mathcal{R}\varphi$ defined on Ω that satisfies $\mathcal{R}\varphi = \varphi$ on Γ and $\mathcal{R}\varphi = 0$ on Σ.

The variational formulation of Problem (3) amounts to the equation (see [19]): Find $E \in \mathcal{H}_t$ such that

$$(\mathcal{A}_t + \mathcal{C}_t) E = F_t, \tag{9}$$

where the operators $\mathcal{A}_t$ and $\mathcal{C}_t : \mathcal{H}_t \to \mathcal{H}_t$ are defined by

$$\begin{aligned}(\mathcal{A}_t E, E')_t \;=\; & \int_\Omega (\operatorname{curl} E \cdot \operatorname{curl} E' + t^{-1} \operatorname{div} E \operatorname{div} E' - k_s^2 E \cdot E') \, d\Omega \\ & + \int_\Sigma (\nu_1 (n_\sigma \times E) \cdot (n_\sigma \times E') + t^{-1} \nu_2 (n_\sigma \cdot E)(n_\sigma \cdot E')) d\sigma,\end{aligned} \tag{10}$$

$$(\mathcal{C}_t E, E')_t = \int_\Sigma (T_{\nu_1} \mathcal{I}_\Gamma^{t,\mathcal{R}} E) \cdot E' d\sigma + t^{-1} \int_\Sigma (N_{\nu_2} \mathcal{I}_\Gamma^{t,\mathcal{R}} E)(n_\sigma \cdot E') d\sigma, \tag{11}$$

and F_t is given by

$$(F_t, E')_t = \int_\Sigma ((T_{\nu_1} E^{inc}) \cdot E' + t^{-1} (N_{\nu_2} E^{inc})(n_\sigma \cdot E')) d\sigma. \tag{12}$$

As explained in [19], Problem (9) is well posed. Moreover, the invertibility of the operator $\mathcal{A}_t$ is equivalently obtained by giving a proof of the uniqueness of the solution of the following problem:

$$\begin{cases} \operatorname{curl} \operatorname{curl} E - t^{-1} \nabla(\operatorname{div} E) - k_s^2 E = 0 \text{ in } \Omega, \\ \operatorname{curl} E \times n + \nu_1 \, n \times (E \times n) = 0 \text{ on } \partial\Omega, \\ \operatorname{div} E + \nu_2 E \cdot n = 0 \text{ on } \partial\Omega, \end{cases} \tag{13}$$

where n is the outward unit normal vector on the boundary $\partial\Omega$, outgoing from Ω. This means that $n = n_\sigma$ on Σ and $n = n_e = -n_\gamma$ on Γ. By a variational formulation, Green's formula, and the boundary conditions on $\partial\Omega$, one can check that

$$\int_\Omega (\operatorname{curl} E \cdot \operatorname{curl} E' + t^{-1} \operatorname{div} E \operatorname{div} E' + k_s^2 E \cdot E') d\Omega + \nu_1 \int_{\partial\Omega} (n \times E) \cdot (n \times E') d\sigma + t^{-1} \nu_2 \int_{\partial\Omega} (n \cdot E)(n \cdot E') d\sigma = 0.$$

Then, choosing $E' = E$, we get $n \times E = 0$ and $n \cdot E = 0$ on $\partial\Omega$. Considering again the boundary conditions: $\operatorname{curl} E \times n = 0$, $\operatorname{div} E = 0$ on $\partial\Omega$ combined to the integral representation of the field solving the first equation of Problem (13) inside a bounded domain ([19]), leads to $E = 0$ in Ω and proves the property:

Property 1.2 *The operator $\mathcal{A}_t$ defined by the expression (10) is invertible.*

Remark 1.3 *If $t \neq \infty$, generally $\mathcal{H}_t \not\subset H^1(\Omega)^3$ [17]. If Ω is a Lipschitz domain with no re-entrant corners, then $\mathcal{H}_t \cap H^1(\Omega)^3$ is dense on $\mathcal{H}_t$ [10]. Thus, we can discretize (9) using Lagrange finite elements. But if the domain has re-entrant corners or edges, $\mathcal{H}_t \cap H^1(\Omega)^3$ is a closed proper subspace of $\mathcal{H}_t$ ([14]). Therefore, $\mathcal{H}_t$ has no dense subspace included in $H^1(\Omega)^3$. In this case, the discretization by Lagrange finite elements of the regularized Maxwell equations leads to a solution that does not converge to the physical*

solution ([11]). In fact in this latter configuration, we can use a weighted regularization method ([13,12]). For the numerical resolution of Problem (2), we restrict ourselves to the case of obstacles without geometrical singularities and such that Ω has no re-entrant corners.

Remark 1.4 *The solution $E \in \mathcal{H}_t$ of Problem (9) satisfies* $\operatorname{curl}\operatorname{curl} E - t^{-1}\nabla(\operatorname{div} E) \in L^2(\Omega)^3$. *Hence, the quantity* $\operatorname{curl} E \times n_\gamma + t^{-1} n_\gamma \operatorname{div} E$ *is defined in $H^{1/2}(\Gamma)^3$ by means of Green's formula. For such a solution E, the integral representation (5) is then as valid as the integral representation (8).*

In the case of the classical Maxwell equations, the weak form of the problem obtained by the application of CEFRI can be derived in a similar way. We just give below the equivalent resulting problem and its variational formulation. By the application of CEFRI, Problem (1) is equivalent to the following problem defined on the bounded domain Ω:

$$\begin{cases} \operatorname{curl}\operatorname{curl} E - k_s^2 E = 0 \text{ in } \Omega, \\ E \times n_\gamma = 0 \text{ on } \Gamma, \\ T_{\nu_1} E = T_{\nu_1}(E^{inc} - \mathcal{I}_\Gamma^\infty E) \text{ on } \Sigma, \end{cases} \tag{14}$$

where $\mathcal{I}_\Gamma^\infty$ is defined in (5) with $t = \infty$. The variational formulation of Problem (14) can be written as: Find $E \in \mathcal{H}_\infty$

$$(\mathcal{A}_\infty + \mathcal{C}_\infty)E = F_\infty, \tag{15}$$

The Hilbert space $\mathcal{H}_\infty$ is given by (6) for $t = \infty$. The operators $\mathcal{A}_\infty$, $\mathcal{C}_\infty$ and F_∞ are respectively defined in (10), (11) and (12) taking $t = \infty$.

2. Schwarz method interpretation

In this section, we first present a resolution strategy for the regularized Maxwell equations. Then, the case of the classical Maxwell equations is briefly considered.

To solve System (9), Jin and Liu [21] suggested to consider $\mathcal{C}_t$, the term containing the integral representation, in the right hand side. An application of the fixed point algorithm leads to finding E_{n+1} such that

$$\begin{cases} \operatorname{curl}\operatorname{curl} E_{n+1} - t^{-1}\nabla(\operatorname{div} E_{n+1}) - k_s^2 E_{n+1} = 0 \text{ in } \Omega, \\ E_{n+1} \times n_\gamma = 0,\ t^{-1}\operatorname{div} E_{n+1} = 0 \text{ on } \Gamma, \\ T_{\nu_1} E_{n+1} = T_{\nu_1}(E^{inc} - \mathcal{I}_\Gamma^t E_n) \text{ on } \Sigma, \\ N_{\nu_2} E_{n+1} = N_{\nu_2}(E^{inc} - \mathcal{I}_\Gamma^t E_n) \text{ on } \Sigma. \end{cases} \tag{16}$$

In this paper, we focus on an original mathematical justification of convergence of the algorithm expressed by Jin and Liu. We interpret the algorithm based on (16) as a Schwarz method. This interpretation has been initially considered for Poisson and Helmholtz problems in [5,6]. The strategy is designated as Total Overlapping Schwarz Method. Indeed the overlapping area is the total domain Ω. We hereby extend this work to the case of Maxwell's equations: it consists in replacing equivalently the problem (16) by the two following subproblems. The first one is a transmission problem in $\mathbb{R}^3$:

$$\begin{cases} \operatorname{curl}\operatorname{curl} E_{2n+1} - t^{-1}\nabla(\operatorname{div} E_{2n+1}) - k_s^2 E_{2n+1} = 0 \text{ in } \Omega_i \cup \Omega_e, \\ n_\gamma \times [E_{2n+1}] = 0,\ n_\gamma \times [\operatorname{curl} E_{2n+1}] = -n_\gamma \times \operatorname{curl} E_{2n} \text{ on } \Gamma, \\ [t^{-1}\operatorname{div} E_{2n+1}] = 0,\ n_\gamma \cdot [t^{-1} E_{2n+1}] = -n_\gamma \cdot t^{-1} E_{2n} \text{ on } \Gamma, \\ \lim\limits_{R\to\infty} \int_{||x||=R} ||\operatorname{curl} E^s_{2n+1} \times n_e - ik_s n_e \times (E^s_{2n+1} \times n_e)||^2 d\gamma = 0, \\ \lim\limits_{R\to\infty} \int_{||x||=R} |\sqrt{t^{-1}}\operatorname{div} E^s_{2n+1} - ik_s E^s_{2n+1} \cdot n_e|^2 d\gamma = 0. \end{cases} \tag{17}$$

The second one consists in finding E_{2n+2} such that

$$\begin{cases} \operatorname{curl}\operatorname{curl} E_{2n+2} - t^{-1}\nabla(\operatorname{div} E_{2n+2}) - k_s^2 E_{2n+2} = 0 \text{ in } \Omega, \\ E_{2n+2} \times n_\gamma = 0,\ t^{-1}\operatorname{div} E_{2n+2} = 0 \text{ on } \Gamma, \\ T_{\nu_1} E_{2n+2} = T_{\nu_1} E_{2n+1} \text{ on } \Sigma, \\ N_{\nu_2} E_{2n+2} = N_{\nu_2} E_{2n+1} \text{ on } \Sigma. \end{cases} \tag{18}$$

The solution E_{2n+1} of (17) has an explicit expression given by an integral representation. By inserting this representation in the right-hand side of the second and third boundary conditions of (18) we effectively obtain the solution of (16). At the iteration n, Schwarz algorithm (Jin and Liu's scheme) is defined by

$$\mathcal{A}_t E^{n+1} = -\mathcal{C}_t E^n + F_t. \tag{19}$$

Numerically, we use the scheme suggested by Jin and Liu and do not use Subproblems (17) and (18). The intermediate problems (17) and (18) are used for theoretical justifications. This allows us to derive convergence estimations that cannot be derived directly from System (16).

Since the operator $\mathcal{A}_t$ is invertible, Equation (19) is equivalent to

$$E^{n+1} = -\mathcal{A}_t^{-1}\mathcal{C}_t E^n + \mathcal{A}_t^{-1} F_t. \tag{20}$$

Both iterative schemes (19) and (20) converge if and only if the spectral radius of ${\mathcal{A}_t}^{-1}\mathcal{C}_t$ is strictly lower than one. This statement shows $\mathcal{A}_t$ as a natural preconditioning of Schwarz method. In the sequel, we designate $\mathcal{A}_t$ as Schwarz preconditioner.

In the case of the classical Maxwell equations, an equivalent strategy can be applied and consists in the consideration of the two following subproblems: The first one consists in finding E_{2n+1} such that

$$\begin{cases} \operatorname{curl}\operatorname{curl} E_{2n+1} - k_s^2 E_{2n+1} = 0 \text{ in } \Omega_i \cup \Omega_e, \\ n_\gamma \times [E_{2n+1}] = 0 \text{ on } \Gamma, \\ n_\gamma \times [\operatorname{curl} E_{2n+1}] = -n_\gamma \times \operatorname{curl} E_{2n} \text{ on } \Gamma, \\ \lim\limits_{R\to\infty} \int_{||x||=R} ||\operatorname{curl} E^s_{2n+1} \times n_e - ik_s E^s_{2n+1}||^2 d\gamma = 0. \end{cases} \tag{21}$$

The other one consists in the following problem: Find E_{2n+2} such that

$$\begin{cases} \text{curl curl} E_{2n+2} - k_s^2 E_{2n+2} = 0 \text{ in } \Omega, \\ E_{2n+2} \times n_\gamma = 0 \text{ on } \Gamma, \\ T_{\nu_1} E_{2n+2} = T_{\nu_1} E_{2n+1} \text{ on } \Sigma. \end{cases} \tag{22}$$

Then, at the iteration n, Schwarz algorithm for the classical Maxwell equations is defined by

$$\mathcal{A}_\infty E^{n+1} = -\mathcal{C}_\infty E^n + F_\infty. \tag{23}$$

Since the operator $\mathcal{A}_\infty$ is invertible, then

$$E^{n+1} = -\mathcal{A}_\infty^{-1}\mathcal{C}_\infty E^n + \mathcal{A}_\infty^{-1} F_\infty. \tag{24}$$

The same statement as for the regularized equations occurs by replacing $\mathcal{A}_t$ and $\mathcal{C}_t$ with $\mathcal{A}_\infty$ and $\mathcal{C}_\infty$.

3. Analytical estimation of the convergence for a spherical scatterer

In this section, we investigate an analytical characterization of the convergence of Schwarz method in a spherical configuration where the scatterer Ω_i is a perfectly conducting ball. The analysis is first presented for the regularized Maxwell equations. Then, using the same approach, we give the corresponding results for the classical Maxwell's equations. The calculation was initially done for the classical Maxwell equations in a way which was not applicable to the regularized equations. At the end of the section, we also reproduce the proof of the rate of convergence in the case of the classical equations in the initial way, which leads to the same convergence estimates.

As a first step, we introduce specific functions based on the Bessel and Hankel functions $J_l(r) = j_l(r) + r j_l'(r)$ and $H_l(r) = h_l(r) + r h_l'(r)$ where j_l (resp. h_l) is the spherical Bessel function (resp. spherical Hankel function of the first kind) of degree l. The following derivation also uses the spherical harmonics Y_l^m, $m = -l, ..., l$, of order $l > 0$.

The special functions of the spherical configuration offer specific properties ([9,24]), with $\hat{x} = x/|x|$:

Proposition 3.1 *Let us consider the regularized Maxwell equation*

$$\text{curl curl E} - \text{t}^{-1}\nabla(\text{div E}) - \text{k}_\text{s}^2\text{E} = 0. \tag{25}$$

Let Y_l^m, $m = -l, ..., l$, be the spherical harmonics of order $l > 0$. The functions

$$M_{lm}(x) = \text{curl}\left\{x\, j_l(k_s|x|)Y_l^m(\hat{x})\right\}, \qquad \widetilde{M}_{lm} = \frac{1}{ik_s}\text{curl}\, M_{lm}, \qquad \widehat{M}_{lm}(x) = \frac{1}{k_p}\nabla(j_l(k_s|x|)Y_l^m(\hat{x}))$$

are solutions of (25) in $\mathbb{R}^3$ and the functions

$$N_{lm}(x) = \text{curl}\left\{x\, h_l(k_s|x|)Y_l^m(\hat{x})\right\}, \qquad \widetilde{N}_{lm} = \frac{1}{ik_s}\text{curl}\, N_{lm}, \qquad \widehat{N}_{lm}(x) = \frac{1}{k_p}\nabla(h_l(k_s|x|)Y_l^m(\hat{x}))$$

are radiating solutions of (25) in $\mathbb{R}^3 \setminus \{0\}$.

Remark 3.2 *For the classical Maxwell equations, a similar result occurs, involving only $M_{lm}, N_{lm}, \widetilde{M}_{lm}$ and $\widetilde{N}_{lm}$ ([27]). For the regularized Maxwell equations, the result is based on some work by Morse and Feshbach ([26]) and $\widehat{M}_{lm}$ and $\widehat{N}_{lm}$ contribute to the irrotational part of the field.*

Proposition 3.3 *If Y_l^m denote the spherical harmonics of order $l > 0$ and $m = -l, ..., l$, then the tangential fields on the unit sphere $\mathcal{S}$*

$$U_{lm} = \frac{1}{\sqrt{l(l+1)}} \nabla_{\mathcal{S}} Y_l^m \quad \textit{and} \quad V_{lm} = n \times U_{lm}$$

are called vector spherical harmonics of order l. The notation $\nabla_{\mathcal{S}}$ denotes the surface gradient on the unit sphere $\mathcal{S}$ and n is the outward unit normal to $\mathcal{S}$. The fields U_{lm} and V_{lm}, l=1,2,3,..., form a complete orthonormal system in the Hilbert space

$$T^2(\mathcal{S}) = \left\{ a : \mathcal{S} \to \mathbb{C}^3 \textit{ such that } a \in L^2(\mathcal{S})^3, a.n = 0 \right\}$$

of square integrable tangential fields on $\mathcal{S}$ equipped with the usual L^2 inner product.

In this analytical investigation, we consider the scatterer to be a ball of radius R_*, we suppose that the artificial boundary Σ is a sphere concentric to Γ with radius $R > R_*$ and we perform the proof in the case where $\nu_1 = \nu_2 = -ik_s$.

3.1. *Characterization of the convergence for the regularized equations*

The exact solution of the regularized exterior Maxwell problem can be written thanks to the functions introduced in Propositions 3.1-3.3 (see for example [9]):

$$E = \sum_{l=1}^{\infty} \sum_{m=-l}^{l} \left(\alpha_{lm} N_{lm} + \beta_{lm} \widetilde{N}_{lm} + \gamma_{lm} \widehat{N}_{lm} \right) + E^{inc}.$$

The error occuring on the field E using Schwarz method is denoted by $(w_n)_n$ and defined by the following expression:

$$w_{2n+1} = \begin{cases} E_{2n+1} - E & \text{in } \Omega_e, \\ E_{2n+1} & \text{in } \Omega_i, \end{cases} \quad \text{and} \quad w_{2n+2} = E_{2n+2} - E \quad \text{in } \Omega,$$

where E_{2n+1} and E_{2n+2} are respectively solutions to (17) and (18). Then, the error on the field E can be written in terms of M_{lm}, N_{lm}, $\widetilde{M}_{lm}$, $\widetilde{N}_{lm}$, $\widehat{M}_{lm}$ and $\widehat{N}_{lm}$:

$$w_{2n+1} = \begin{cases} \displaystyle\sum_{l=1}^{\infty} \sum_{m=-l}^{l} \left(a_{lm}^{2n+1} M_{lm} + \widetilde{a}_{lm}^{2n+1} \widetilde{M}_{lm} + \widehat{a}_{lm}^{2n+1} \widehat{M}_{lm} \right), \ |x| \leq R_*, \\ \displaystyle\sum_{l=1}^{\infty} \sum_{m=-l}^{l} \left(b_{lm}^{2n+1} N_{lm} + \widetilde{b}_{lm}^{2n+1} \widetilde{N}_{lm} + \widehat{b}_{lm}^{2n+1} \widehat{N}_{lm} \right), \ |x| > R_*, \end{cases}$$

$$w_{2n+2} = \sum_{l=1}^{\infty} \sum_{m=-l}^{l} \left(c_{lm}^{2n+2} M_{lm} + d_{lm}^{2n+2} N_{lm} + \widetilde{c}_{lm}^{2n+2} \widetilde{M}_{lm} + \widetilde{d}_{lm}^{2n+2} \widetilde{N}_{lm} + \widehat{c}_{lm}^{2n+2} \widehat{M}_{lm} + \widehat{d}_{lm}^{2n+2} \widehat{N}_{lm} \right).$$

As a first step, we interpret the boundary conditions on Γ and on Σ. Some conditions give relations between coefficients such that the number of significant coefficients is reduced:

- ⋆ the coefficients $\left(c_{lm}^{2n+2}, \widetilde{c}_{lm}^{2n+2}, \widehat{c}_{lm}^{2n+2}\right)$ are uniquely expressed thanks to $\left(d_{lm}^{2n+2}, \widetilde{d}_{lm}^{2n+2}, \widehat{d}_{lm}^{2n+2}\right)$ (let us remark that the same link is valid at the level iteration $2n$);
- ⋆ an equivalent statement occurs between $\left(a_{lm}^{2n+1}, \widetilde{a}_{lm}^{2n+1}, \widehat{a}_{lm}^{2n+1}\right)$ and $\left(b_{lm}^{2n+1}, \widetilde{b}_{lm}^{2n+1}, \widehat{b}_{lm}^{2n+1}\right)$.

The other conditions give the ingredients for the characterization of the convergence:

$\star$ a relation expresses $\left(b_{lm}^{2n+1}, \widetilde{b}_{lm}^{2n+1}, \widehat{b}_{lm}^{2n+1}\right)$ from $\left(d_{lm}^{2n}, \widetilde{d}_{lm}^{2n}, \widehat{d}_{lm}^{2n}\right)$;

$\star$ a relation gives $\left(d_{lm}^{2n+2}, \widetilde{d}_{lm}^{2n+2}, \widehat{d}_{lm}^{2n+2}\right)$ from $\left(b_{lm}^{2n+1}, \widetilde{b}_{lm}^{2n+1}, \widehat{b}_{lm}^{2n+1}\right)$.

A strategy to characterize the convergence consists in introducing the quantity

$$\Lambda_n = \begin{pmatrix} T_{\nu_1}(w_{2n}) \\ N_{\nu_2}(w_{2n}) \end{pmatrix}$$

and study the relation between Λ_n and Λ_{n+1} which corresponds equivalently to the relation between the vectors of coefficients $\left(d_{lm}^{2n+2}, \widetilde{d}_{lm}^{2n+2}, \widehat{d}_{lm}^{2n+2}\right)$ and $\left(d_{lm}^{2n}, \widetilde{d}_{lm}^{2n}, \widehat{d}_{lm}^{2n}\right)$. Let us denote $\widetilde{K}_r$ the operator which maps $\left(d_{lm}^{2n}, \widetilde{d}_{lm}^{2n}, \widehat{d}_{lm}^{2n}\right)$ onto $\left(d_{lm}^{2n+2}, \widetilde{d}_{lm}^{2n+2}, \widehat{d}_{lm}^{2n+2}\right)$. The previous statements lead to the following result: using the notations

$$\begin{aligned}
&H_l(k_s|x|) = h_l(k_s|x|) + k_s|x|h_l'(k_s|x|), \quad J_l(k_s|x|) = j_l(k_s|x|) + k_s|x|j_l'(k_s|x|),\\
&\alpha_l(k_sR) = J_l(k_sR) - ik_sRj_l(k_sR), \quad \beta_l(k_sR) = H_l(k_sR) - ik_sRh_l(k_sR),\\
&H_l^{\sqrt{t}} = h_l(k_sR) - i\sqrt{t}h_l'(k_sR), \quad J_l^{\sqrt{t}} = j_l(k_sR) + i\sqrt{t}j_l'(k_sR),\\
&\gamma_l^* = \frac{H_l(k_sR_*)}{J_l(k_sR_*)}, \quad \delta_l^* = \frac{h_l(k_sR_*)}{j_l(k_sR_*)},
\end{aligned}$$

we have the relation

$$A_r \begin{pmatrix} d_{lm}^{2n+2} \\ \widetilde{d}_{lm}^{2n+2} \\ \widehat{d}_{lm}^{2n+2} \end{pmatrix} = B_r \begin{pmatrix} d_{lm}^{2n} \\ \widetilde{d}_{lm}^{2n} \\ \widehat{d}_{lm}^{2n} \end{pmatrix} \tag{26}$$

where

$$A_r = \begin{pmatrix} 0 & \beta_l(k_sR) - \gamma_l^*\alpha_l(k_sR) & -\frac{i}{\sqrt{t}}\left(\gamma_l^* j_l(k_sR) - h_l(k_sR)\right) \\ \beta_l(k_sR) - \gamma_l^*\alpha_l(k_sR) & 0 & 0 \\ 0 & \frac{-\sqrt{t}l(l+1)}{R}\left(h_l(k_sR) - \gamma_l^* j_l(k_sR)\right) & \frac{k_p}{t}\left(-H_l^{\sqrt{t}} + \gamma_l^* J_l^{\sqrt{t}}\right) \end{pmatrix}$$

and

$$B_r = \begin{pmatrix} 0 & \beta_l(k_sR) & \frac{i}{\sqrt{t}}h_l(k_sR) \\ \beta_l(k_sR) & 0 & 0 \\ 0 & \frac{-\sqrt{t}l(l+1)}{R}h_l(k_sR) & -\frac{k_p}{t}\left(h_l(k_sR) + i\sqrt{t}h_l'(k_sR)\right) \end{pmatrix}.$$

As a consequence, the rate of convergence of the Total Overlapping Schwarz method is given by the spectral radius of $A_r^{-1}B_r$. The method converges when this spectral radius is strictly lower than 1. In the case of the classical Maxwell equations, we give the asymptotic behavior of the spectral radius with respect to the degree l (see Sections 3.2 and 3.3). In the current context of the regularized equations, we just illustrate the behavior of $\rho(\widetilde{K}_r)$ the spectral radius of $\widetilde{K}_r = A_r^{-1}B_r$ with respect to the geometrical,

physical and regularization parameters: the thickness $R - R^*$, wavenumber k_s, wavelength $\lambda_s = 2\pi/k_s$ and regularization parameter t.

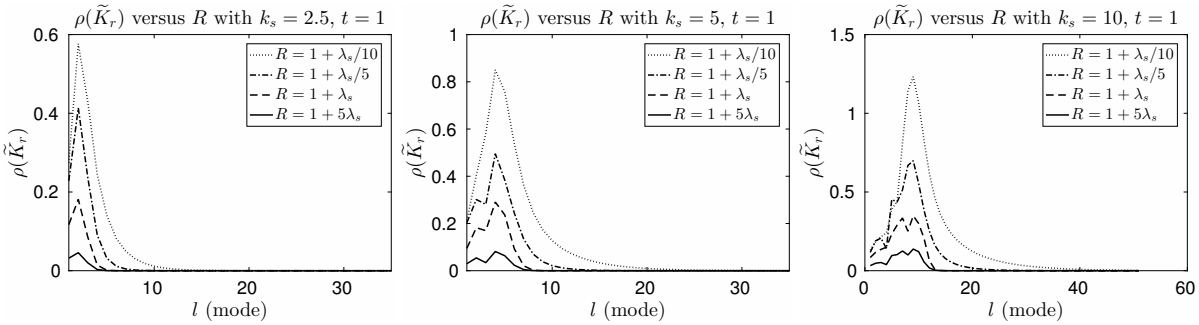

Figure 1. The spectral radius of $\widetilde{K}_r$ vs the thickness of the domain, for $k_s = 2.5$ (left), $k_s = 5$ (center) and $k_s = 10$ (right), with $t = 1$.

Figure 1 indicates for the first values of l how $\rho(\widetilde{K}_r)$ is behaving with respect to the thickness of the computational domain Ω when t is given equal to 1 and when k_s takes three different values (2.5, 5, 10). For all these values of k_s, one can observe that larger is $R - R^*$, smaller is the spectral radius. Figure 2

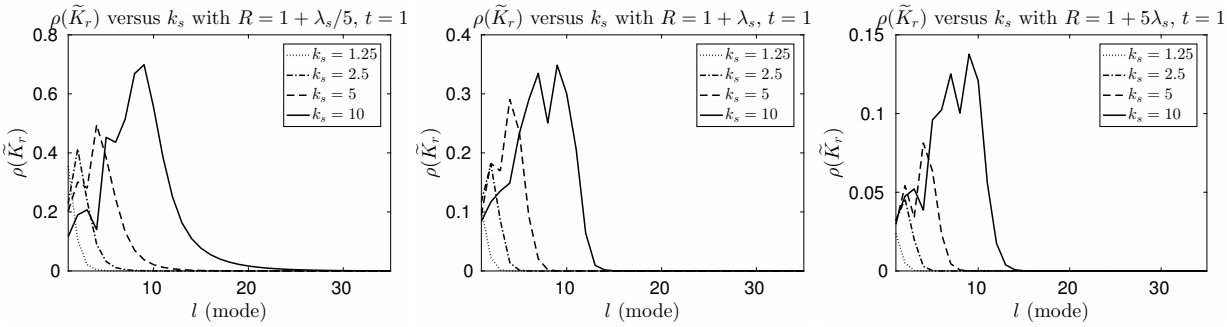

Figure 2. The spectral radius of $\widetilde{K}_r$ vs the wavenumber k_s, for $R = R^* + \lambda_s/5$ (left), $R = R^* + \lambda_s$ (center) and $R = R^* + 5\lambda_s$ (right), with $t = 1$.

indicates for the first values of l how $\rho(\widetilde{K}_r)$ is behaving with respect to the wavenumber k_s when t is given equal to 1 and when $R - R^*$ takes different values with respect to the wavelength ($\lambda_s/5$, λ_s, $5\lambda_s$). For all these values of $R - R^*$, we can see that the quantity $\rho(\widetilde{K}_r)$ is rather deteriorated when the wavenumber increases. Figures 3-4 give for the first values of l the behavior of $\rho(\widetilde{K}_r)$ with respect to the regularization parameter t when the wavenumber k_s takes the value 5, and $R - R^*$ takes the values ($\lambda_s/5$, λ_s, $5\lambda_s$). These observations advise a choice of t of order of the unity. The same behavior was observed for $k_s = 2.5$ and $k_s = 10$.

3.2. *Rate of convergence for the classical equations*

We now adapt the results of Section 3.1 to the classical Maxwell equations. In this context, thanks to Remark 3.2, the calculation does not involve $\widehat{M}_{lm}$ and $\widehat{N}_{lm}$ anymore. By the same strategy as the one in Section 3.1, the rate of convergence is given by the spectral radius of matrix $A_c^{-1}B_c$ where the matrix A_c (respectively B_c) is one diagonal 2×2 block of the matrix A_r (respectively B_r) and

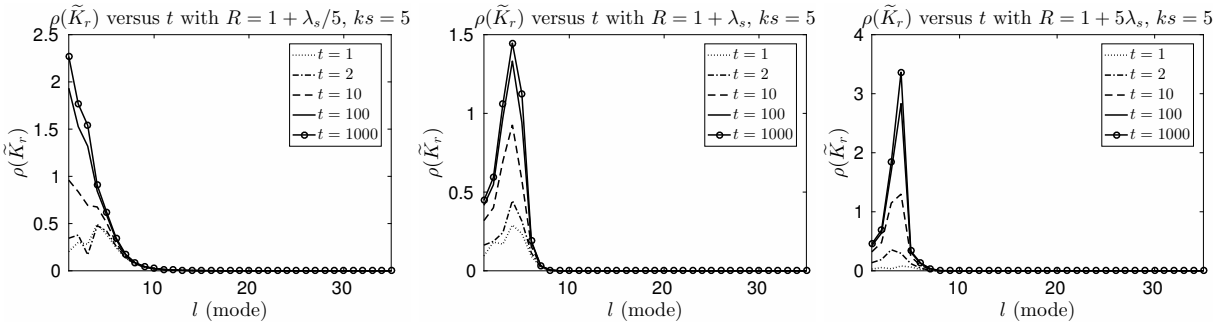

Figure 3. The spectral radius of $\widetilde{K}_r$ vs the regularization parameter t, for $R = R^* + \lambda_s/5$ (left), $R = R^* + \lambda_s$ (center) and $R = R^* + 5\lambda_s$ (right), with $k_s = 5$.

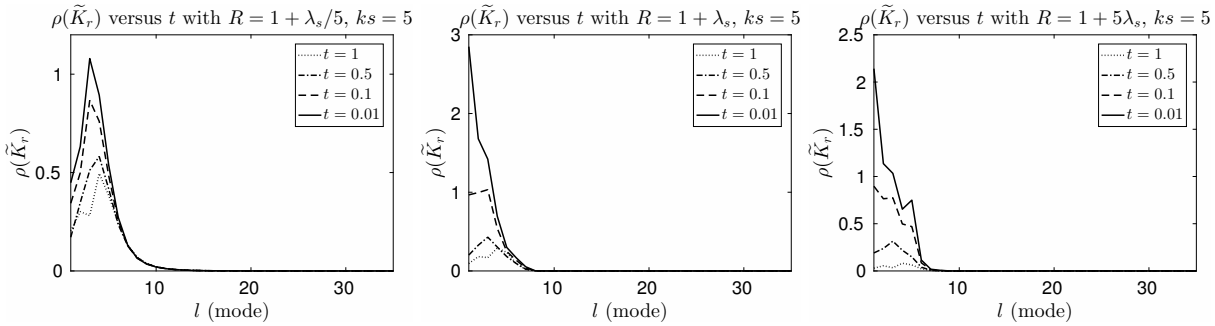

Figure 4. The spectral radius of $\widetilde{K}_r$ vs the regularization parameter t, for $R = R^* + \lambda_s/5$ (left), $R = R^* + \lambda_s$ (center) and $R = R^* + 5\lambda_s$ (right), with $k_s = 5$.

$$A_c^{-1}B_c = \begin{pmatrix} \left(1 - \dfrac{h_l(k_sR_*)}{j_l(k_sR_*)}\ \dfrac{J_l(k_sR) - ik_sRj_l(k_sR)}{H_l(k_sR) - ik_sRh_l(k_sR)}\right)^{-1} & 0 \\ 0 & \left(1 - \dfrac{H_l(k_sR_*)}{J_l(k_sR_*)}\ \dfrac{J_l(k_sR) - ik_sRj_l(k_sR)}{H_l(k_sR) - ik_sRh_l(k_sR)}\right)^{-1} \end{pmatrix}. \quad (27)$$

For the classical equations, the Total Overlapping Schwarz method converges if the spectral radius $\rho(A_c^{-1}B_c)$ of $A_c^{-1}B_c$ is strictly lower than 1. For $R_* = 1$, the asymptotic behavior of the spherical Bessel functions leads to the asymptotic estimation: for large l,

$$\rho(A_c^{-1}B_c) \sim \frac{1}{R^{2l} - 1}\ , \quad i = 1, 2. \quad (28)$$

As a consequence, there might be a finite number of modes (corresponding to some values of l) outside of the unit disk for any value of R depending on the wavenumber. Illustrations are given in Section 3.3 where the same result is obtained using a different strategy. The figures show the behavior of the eigenvalues of the iteration matrix with respect to the wavelength k_s and radius R.

3.3. *Rate of convergence for the classical equations – the initial derivation*

Here, we propose a second strategy to calculate the rate of convergence of Schwarz method for the classical equations. This strategy was indeed the initial one but not extendible to the regularized equations.

For all n, we define $\widetilde{\Lambda}_n = T_{\nu_1}(w_{2n})$. In order to estimate the convergence of the error $(w_{2n})_n$, we study the convergence of $(\widetilde{\Lambda}_n)_n$ considering that $\widetilde{\Lambda}_{n+1} = \widetilde{K}_c\widetilde{\Lambda}_n$ with $\widetilde{K}_c$ a map to be determined from $T^2(\Sigma)$ to

$T^2(\Sigma)$, where $T^2(\Sigma)$ is defined in Proposition 3.3. The quantity $\widetilde{\Lambda}_n$ can be expressed on the basis of the vector spherical harmonics as follows (again due to Proposition 3.3), using the coefficients introduced in Section 3.1:

$$\begin{aligned}\widetilde{\Lambda}_n &= T_{\nu_1}(w_{2n}) = \sum_{l=1}^{\infty}\sum_{m=-l}^{l}\left(c_{lm}^{2n}T_{\nu_1}(M_{lm}) + d_{lm}^{2n}T_{\nu_1}(N_{lm}) + \widetilde{c}_{lm}^{2n}T_{\nu_1}(\widetilde{M}_{lm}) + \widetilde{d}_{lm}^{2n}T_{\nu_1}(\widetilde{N}_{lm})\right)\\ &= \sum_{l,m}\lambda_{lm}^{1,n}\,U_{lm} + \lambda_{lm}^{2,n}\,V_{lm}\,.\end{aligned}$$

The relations between $\widetilde{\Lambda}_n$ and $\widetilde{\Lambda}_{n+1}$ given by conditions on Σ and Γ induce the following statement on the components $\lambda_{lm}^{1,n}$ and $\lambda_{lm}^{2,n}$

$$\begin{cases}\lambda_{lm}^{1,n+1} = \tau_{1,lm}\,\lambda_{lm}^{1,n},\\ \\ \lambda_{lm}^{2,n+1} = \tau_{2,lm}\,\lambda_{lm}^{2,n},\end{cases}$$

where

$$\begin{cases}\tau_{1,lm} = \left(\dfrac{\tilde{d}_{lm}^{2n}}{\widetilde{b}_{lm}^{2n+1}} + \dfrac{\tilde{c}_{lm}^{2n}}{\widetilde{b}_{lm}^{2n+1}}\,\dfrac{ik_sJ_l(k_sR)+k_s^2Rj_l(k_sR)}{ik_sH_l(k_sR)+k_s^2Rh_l(k_sR)}\right)^{-1},\\ \\ \tau_{2,lm} = \left(\dfrac{d_{lm}^{2n}}{b_{lm}^{2n+1}} + \dfrac{c_{lm}^{2n}}{b_{lm}^{2n+1}}\,\dfrac{J_l(k_sR)-ik_sRj_l(k_sR)}{H_l(k_sR)-ik_sRh_l(k_sR)}\right)^{-1}.\end{cases}$$

These expressions clearly indicate that $\widetilde{K}_c$ is linear and has a diagonal representation in the basis $\{U_{lm}, V_{lm}, l\in\mathbb{N}, m=-l,...,l\}$ of $T^2(\Sigma)$. The relation between $(b_{lm}^{2n+1}, \widetilde{b}_{lm}^{2n+1})$ and $(d_{lm}^{2n+1}, \widetilde{d}_{lm}^{2n+1})$ leads to

$$\begin{cases}\tau_{1,lm} = \left(1 - \dfrac{H_l(k_sR_*)}{J_l(k_sR_*)}\,\dfrac{J_l(k_sR)-ik_sRj_l(k_sR)}{H_l(k_sR)-ik_sRh_l(k_sR)}\right)^{-1},\\ \\ \tau_{2,lm} = \left(1 - \dfrac{h_l(k_sR_*)}{j_l(k_sR_*)}\,\dfrac{J_l(k_sR)-ik_sRj_l(k_sR)}{H_l(k_sR)-ik_sRh_l(k_sR)}\right)^{-1}.\end{cases}\tag{29}$$

The spectrum of $\widetilde{K}_c$ consists of the eigenvalues $\tau_{1,lm}$ and $\tau_{2,lm}$. Their explicit derivation indicates that these quantities are independent of m. Let us denote them $\tau_{1,l}$ and $\tau_{2,l}$ in the sequel. These eigenvalues define the rate of convergence of the Schwarz method. Then, the convergence of the Total Overlapping Schwarz method is ensured if $|\tau_{i,l}| < 1$, for all $i = 1, 2$, for all $l \in \mathbb{N}$. Relations (27) and (29) are similar which indicates that the result is given by the estimation (28).

Let us now illustrate the eigenvalues $\tau_{1,l}$ and $\tau_{2,l}$ for different values of R. Figures 5, 6 indicate how $\tau_{1,:}$ and $\tau_{2,:}$ behave with respect to the thickness of the computational domain Ω when k_s takes three different values (2.5, 5, 10). Figures 7, 8 indicate how $\tau_{1,:}$ and $\tau_{2,:}$ behave with respect to the wavenumber k_s when $R - R^*$ takes different values with respect to the wavelength ($\lambda_s/5$, λ_s, $5\lambda_s$).

3.4. *Motivation of Schwarz preconditioner*

Due to the observed limitations (the requirements on the thickness of the computational domain, the behavior with respect to the wavenumber), a Krylov method appears as a relevant alternative to the algorithm defined by (16): due to the properties of Krylov solvers demonstrated in [18], the convergence of a Krylov method is ensured for the resolution of Problem (9) using $\mathcal{A}_t$ as a preconditioner. Such a strategy consists in solving the system

$$(I + \mathcal{A}_t^{-1}\mathcal{C}_t)E = \mathcal{A}_t^{-1}F_t \tag{30}$$

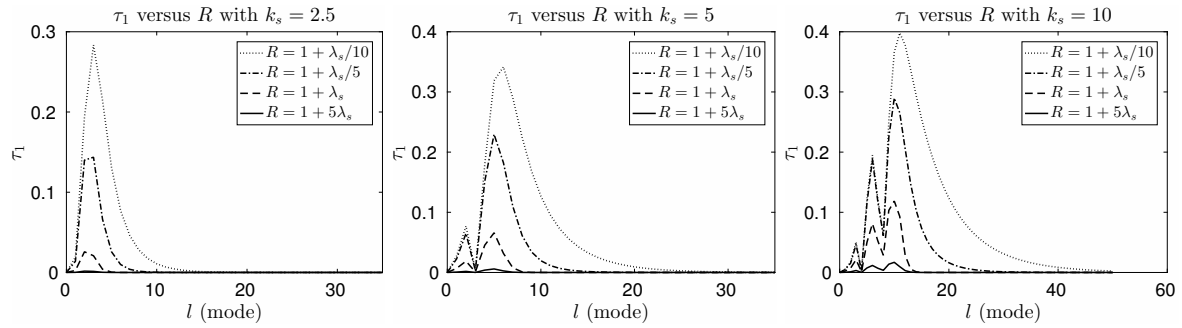

Figure 5. The value of $\tau_{1,:}$ vs the thickness of the domain, for $k_s = 2.5$ (left), $k_s = 5$ (center) and $k_s = 10$ (right).

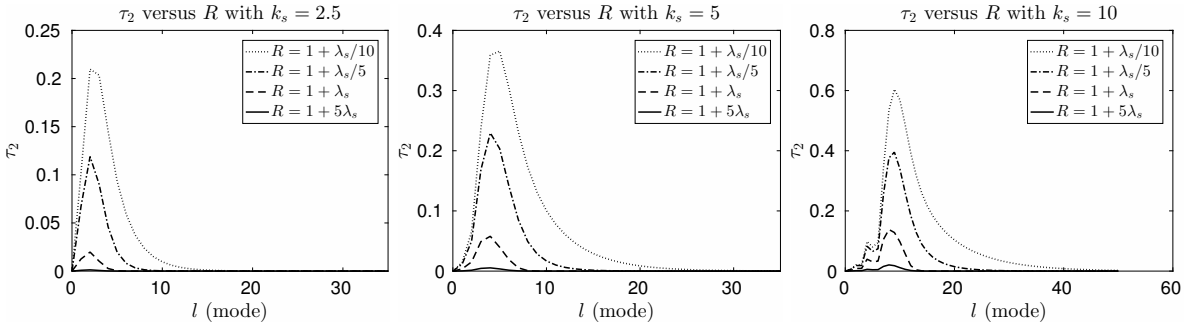

Figure 6. The value of $\tau_{2,:}$ vs the thickness of the domain, for $k_s = 2.5$ (left), $k_s = 5$ (center) and $k_s = 10$ (right).

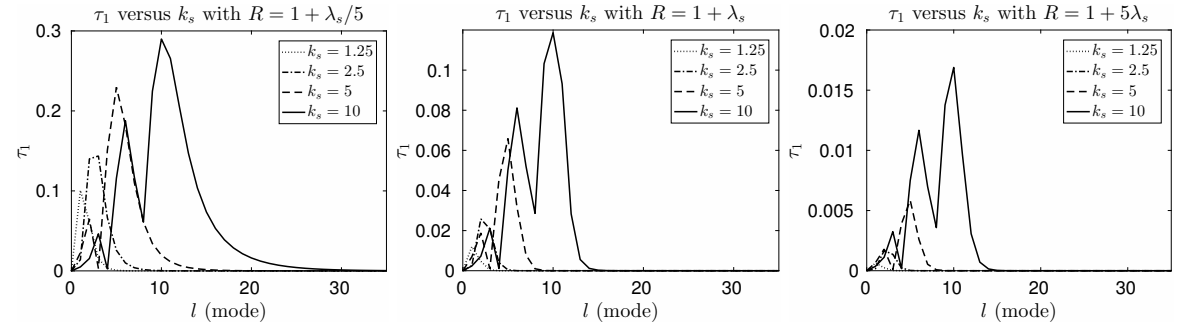

Figure 7. The value of $\tau_{1,:}$ vs the wavenumber k_s, for $R = R^* + \lambda_s/5$ (left), $R = R^* + \lambda_s$ (center) and $R = R^* + 5\lambda_s$ (right).

by a Krylov method. As a first statement, the convergence of an iterative method applied to Problem (30) is ensured if the spectral radius of $(\mathcal{A}_t^{-1}\mathcal{C}_t)$ is lower than 1. This condition is exactly the condition of convergence of Jin and Liu scheme considered in the previous sections. This specifies how the analysis of Schwarz algorithm suggests such a preconditioning strategy for a Krylov solver approach. However, the properties established in [18] indicates that the convergence of GMRES for the resolution of Problem (30) is ensured even if some eigenvalues of $\mathcal{A}_t^{-1}\mathcal{C}_t$ have a modulus larger than one. Hence, the Krylov method can achieve convergence even in the case of thin domain of computation Ω. In the next sections, we study theoretically and numerically the convergence of GMRES applied to Problem (9) using $\mathcal{A}_t$ as a preconditioner.

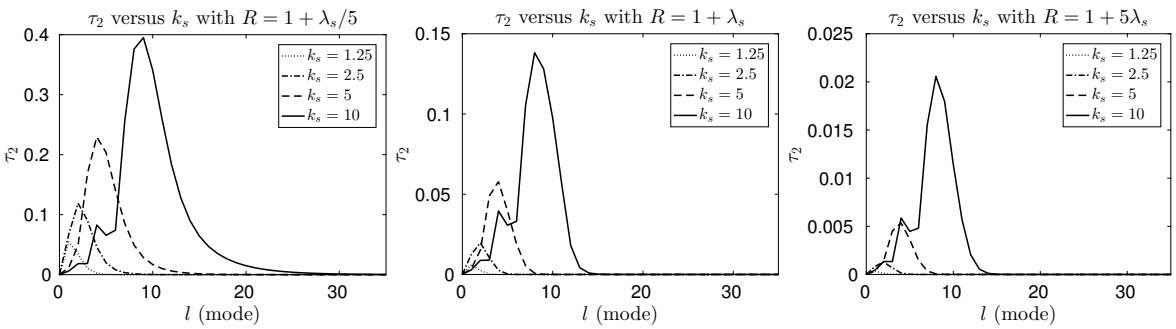

Figure 8. The value of $\tau_{2,:}$ vs the wavenumber k_s, for $R = R^* + \lambda_s/5$ (left), $R = R^* + \lambda_s$ (center) and $R = R^* + 5\lambda_s$ (right).

4. Convergence analysis for GMRES

In this section, we consider the convergence of GMRES for the resolution of Problem (30) in a spherical configuration. The idea of the proof was initially introduced by F. Ben Belgacem et al [6] for Helmholtz problem: The authors proved the superlinear convergence of GMRES using results of spectral theory. The equation (30) is posed on the domain Ω. We hereby answer the question by considering an intermediate equivalent problem which involves an equation posed on Σ. The rate of convergence of GMRES is similar for both the intermediate equation posed on Σ and the initial problem (30). The difference lies only in the storage size of the Arnoldi basis of GMRES, which is justified later.

To derive the equivalent intermediate problem, we introduce Ψ defined on Σ as a new unknown:

$$\Psi(x) = \Lambda(x) + t^{-1}\, n_\sigma \lambda(x) \qquad \forall\, x \in \Sigma \tag{31}$$

where

$$\Lambda = T_{\nu_1}(E^{inc} - \mathcal{I}_\Gamma^{t,\mathcal{R}} E)$$

and

$$\lambda = N_{\nu_2}(E^{inc} - \mathcal{I}_\Gamma^{t,\mathcal{R}} E).$$

Problem (3) can be written as follows

$$\begin{cases} \operatorname{curl}\operatorname{curl} E - t^{-1}\nabla(\operatorname{div} E) - k_s^2 E = 0 \text{ in } \Omega, \\ E \times n_\gamma = 0, t^{-1}\operatorname{div} E = 0 \text{ on } \Gamma, \\ \operatorname{curl} E \times n_\sigma + \nu_1 n_\sigma \times (E \times n_\sigma) = \Lambda \text{ on } \Sigma, \\ \operatorname{div} E + \nu_2\, E \cdot n_\sigma = \lambda \text{ on } \Sigma. \end{cases} \tag{32}$$

The variational formulation of Problem (32) is

$$\mathcal{A}_t E - \mathcal{D}_t \Psi = 0 \tag{33}$$

where $\mathcal{D}_t$ is defined by

$$(\mathcal{D}_t \Psi, E')_t = \int_\Sigma \Psi \cdot E' d\sigma.$$

We introduce the operator $\mathcal{B}_\Gamma$ which links the two unknowns Ψ and E

$$\mathcal{B}_\Gamma(\Psi) = T_{\nu_1}\mathcal{I}_\Gamma^{t,\mathcal{R}} E + t^{-1}(N_{\nu_2}\mathcal{I}_\Gamma^{t,\mathcal{R}} E) n_\sigma$$

such that the unknown Ψ can be obtained as the solution of a problem defined on Σ

$$\Psi(x) + \mathcal{B}_\Gamma(\Psi)(x) = T_{\nu_1} E^{inc} + t^{-1}(N_{\nu_2} E^{inc}) n_\sigma \qquad \forall\, x \in \Sigma.$$

or equivalently

$$(\mathcal{I} + \mathcal{B}_\Gamma)\Psi = \widetilde{\mathcal{F}}_t \text{ on } L^2(\Sigma)^3, \tag{34}$$

where $\widetilde{\mathcal{F}}_t$ is given by the Riesz representation theorem.

Therefore, the initial problem (30) is equivalent to the combination of the equations (33-34). The rate of convergence of GMRES for Problem (30) is given by the rate of convergence of GMRES for the resolution of Equation (34) which we investigate below.

Lemma 4.1 *The rate of convergence of GMRES for Problem (30) posed in Ω is given by the rate of convergence of GMRES for the resolution of Equation (34) defined on Σ.*

Proof: Let W_{n+1} (resp. $\widetilde{W}_{n+1}$) be the error on the solution E (resp. on the field Ψ) of Problem (30) (resp. (34)) at iteration $n+1$ of the GMRES method. Then, the error W_{n+1} satisfies the following system on W

$$\begin{cases} \text{curl curl}\, W - t^{-1}\nabla(\text{div}\, W) - k_s^2 W = 0 \text{ in } \Omega, \\ W \times n_\gamma = 0, t^{-1}\text{div}\, W = 0 \text{ on } \Gamma, \\ T_{\nu_1} W = \tilde{\Lambda} \text{ on } \Sigma, \\ N_{\nu_2} W = \tilde{\lambda} \text{ on } \Sigma. \end{cases} \tag{35}$$

when

$$\tilde{\Lambda} = -T_{\nu_1}\mathcal{I}_\Gamma^{t,\mathcal{R}} W_n \quad \text{and} \quad \tilde{\lambda} = -N_{\nu_2}\mathcal{I}_\Gamma^{t,\mathcal{R}} W_n.$$

If $\mathcal{B}_\Omega$ denotes $\mathcal{A}_t^{-1}\mathcal{C}_t$ the iteration matrix of GMRES solver for Problem (30), then at each iteration

$$W_{n+1} = \mathcal{B}_\Omega W_n\,. \tag{36}$$

The same relation holds for $\widetilde{W}_{n+1}$

$$\widetilde{W}_{n+1} = \mathcal{B}_\Gamma \widetilde{W}_n\,. \tag{37}$$

Now, let us consider the two linear maps

$$\begin{aligned} \Phi : T^2(\Sigma) \times L^2(\Sigma) &\to \mathcal{H}_t \\ (\tilde{\Lambda}, \tilde{\lambda}) &\mapsto W \end{aligned}$$

where W is the solution of System (35), and

$$\begin{aligned} \tilde{\Phi} : T^2(\Sigma) \times L^2(\Sigma) &\to L^2(\Sigma)^3 \\ (\tilde{\Lambda}, \tilde{\lambda}) &\mapsto \widetilde{W} = \tilde{\Lambda} + t^{-1}\, n_\sigma \tilde{\lambda} \end{aligned}$$

related to Definition (31). The linear map Φ is invertible due to the well posedness of the associated problem (35) and $\tilde{\Phi}$ is invertible due to orthogonality arguments. These definitions lead to

$$W_{n+1} = \Phi\tilde{\Phi}^{-1}\widetilde{W}_{n+1} \tag{38}$$

By the equations (36) and (38), we then have

$$\widetilde{W}_{n+1} = \tilde{\Phi}\Phi^{-1}\mathcal{B}_\Omega\Phi\tilde{\Phi}^{-1}\widetilde{W}_n. \tag{39}$$

and this holds for any first iterate $\widetilde{W}_0$. Combining (37) and (39), we can conclude that

$$\mathcal{B}_\Gamma = \tilde{\Phi}\Phi^{-1}\mathcal{B}_\Omega\Phi\tilde{\Phi}^{-1}.$$

We deduce that the eigenvalues of $\mathcal{B}_\Gamma$ are eigenvalues of $\mathcal{B}_\Omega$. □

Thanks to the previous statement, we now focus on the convergence of GMRES for Problem (34). From [19], one can check that $\mathcal{B}_\Gamma$ is a continuous operator from $L^2(\Sigma)^3$ to $\mathcal{H}_t$. Moreover, the injection $\mathcal{H}_t \hookrightarrow L^2(\Omega)^3$ is compact ([19]). Thus, the injection $\mathcal{H}_t \hookrightarrow L^2(\Sigma)^3$ is also compact. This implies that $\mathcal{B}_\Gamma$ is a compact operator on $L^2(\Sigma)^3$. Due to the work by I. Moret [25], the convergence of GMRES for the resolution of Problem (34) is ensured. In the following, we precise the rate of convergence by verifying the exponential decay of each singular value γ_p, $p \geq 0$ of $\mathcal{B}_\Gamma$.

Proposition 4.2 *In the case of a spherical scatterer, with a spherical artificial boundary, there exist two positive constants c and τ such that the singular values of $\mathcal{B}_\Gamma$, γ_p, $p \geq 0$, satisfy the relation*

$$0 \leq \gamma_p \leq c\, \mathrm{e}^{-\tau\sqrt{p}}, \qquad \forall\, p \geq 0.$$

Proof: The proof of the proposition is performed for the case where the scatterer is a perfectly conducting ball with radius $R_* = 1$ and the artificial boundary Σ is the sphere concentric to Γ with radius $R > R_*$.

The first step of the convergence evaluation consists in constructing an operator $(\mathcal{B}_\Gamma)_p$ with rank $\leq p$ which approximates $\mathcal{B}_\Gamma$. The proof is based on the Courant-Weyl min-max principle [29] together with an expansion in term of Bessel and Hankel functions and harmonic spherical functions. We perform the proof in the case $\nu_1 = \nu_2 = -ik_s$.. We recall that the Green's function associated with the 3D Helmholtz equation can be written as follows ([9]) :

$$G_{k_s}(x,y) = ik_s \sum_{l=0}^{\infty} \sum_{m=-l}^{l} h_l(k_s|x|) Y_l^m(\hat{x}) j_l(k_s|y|) \overline{Y_l^m(\hat{y})}, \tag{40}$$

with $\hat{x} = x/|x|$ and $\hat{y} = y/|y|$. The series (40) and its term by term first derivatives with respect to x and y are absolutely and uniformly convergent on compact subsets of $\{(x,y) \in \mathbb{R}^3 \times \mathbb{R}^3 \ ; \ |x| > |y|\}$ (in our use of the relation, x is on Σ and y is on Γ). Moreover, if V is a given vector, the following expansion holds ([9])

$$\begin{aligned} G_{k_s}(x,y)V \ = & \ \frac{i}{k_s} \sum_{l=1}^{\infty} \frac{1}{l(l+1)} \sum_{m=-l}^{l} \operatorname{curl} N_{lm}(x)\, \overline{\operatorname{curl} M_{lm}(y)} \cdot V \\ & + ik_s \sum_{l=1}^{\infty} \frac{ik_s}{l(l+1)} \sum_{m=-l}^{l} N_{lm}(x)\, \overline{M_{lm}(y)} \cdot V \\ & + \frac{i}{k_s} \sum_{l=1}^{\infty} \sum_{m=-l}^{l} \nabla(h_l(k_s|x|) Y_l^m(\hat{x}))\, \overline{\nabla(j_l(k_s|y|) Y_l^m(\hat{y}))} \cdot V\,. \end{aligned} \tag{41}$$

The series (41) and its term by term derivatives in x and y are uniformly and absolutely convergent on compact subsets of $\{(x,y) \in \mathbb{R}^3 \times \mathbb{R}^3 \ ; \ |x| > |y|\}$ ([9], [24]). The integral representation (5) can be written as follows:

$$(\mathcal{I}_\Gamma^t E)(x) = \operatorname{curl}_x \operatorname{curl}_x \int_\Gamma G_{k_s}(x,y)(\operatorname{curl} E(y) \times n_\gamma(y)) d\gamma(y) - \int_\Gamma \nabla_y G_{k_p}(x,y)(E(y) \cdot n_\gamma(y)) d\gamma(y).$$

Then, taking the formulas (40) and (41) into account, we have, for all $x \in \Omega_e$

$$\begin{aligned} (\mathcal{I}_\Gamma^t E)(x) \ = & \ \operatorname{curl}_x \operatorname{curl}_x \int_\Gamma \frac{i}{k_s} \sum_{l=1}^{\infty} \frac{1}{l(l+1)} \sum_{m=-l}^{l} \operatorname{curl} N_{lm}(x)\, \overline{\operatorname{curl} M_{lm}(y)} \cdot (\operatorname{curl} E(y) \times n_\gamma(y)) d\gamma(y) \\ & + \operatorname{curl}_x \operatorname{curl}_x \int_\Gamma ik_s \sum_{l=1}^{\infty} \frac{1}{l(l+1)} \sum_{m=-l}^{l} N_{lm}(x)\, \overline{M_{lm}(y)} \cdot (\operatorname{curl} E(y) \times n_\gamma(y)) d\gamma(y) \\ & + ik_p \int_\Gamma \sum_{l=0}^{\infty} \sum_{m=-l}^{l} j_l(k_p|y|) \overline{Y_l^m(\hat{y})} (k_p\, \hat{x}\, h_l'(k_p|x|) Y_l^m(\hat{x}) + h_l(k_p|x|) \frac{1}{|x|} \nabla_{\mathcal{S}} Y_l^m(\hat{x}))(E(y) \cdot n_\gamma(y)) d\gamma(y). \end{aligned}$$

Thus, the operator $\mathcal{B}_\Gamma$ can be written as follows: for all $x \in \Sigma$

$$
\begin{aligned}
\mathcal{B}_\Gamma \Psi(x) = & \int_\Gamma \sum_{l=1}^{\infty} \frac{ik_s^3}{l(l+1)} \sum_{m=-l}^{l} (N_{lm}(x) \times n_\sigma(x)) \ \overline{\operatorname{curl} M_{lm}(y)} \cdot (\operatorname{curl} E(y) \times n_\gamma(y)) d\gamma(y) \\
& + \int_\Gamma \sum_{l=1}^{\infty} \frac{ik_s^3}{l(l+1)} \sum_{m=-l}^{l} (\operatorname{curl} N_{lm}(x) \times n_\sigma(x)) \, \overline{M_{lm}(y)} \cdot (\operatorname{curl} E(y) \times n_\gamma(y)) d\gamma(y) \\
& + \int_\Gamma \sum_{l=1}^{\infty} \frac{k_s^2}{l(l+1)} \sum_{m=-l}^{l} (n_\sigma(x) \times (\operatorname{curl} N_{lm}(x) \times n_\sigma(x))) \, \overline{\operatorname{curl} M_{lm}(y)} \cdot (\operatorname{curl} E(y) \times n_\gamma(y)) d\gamma(y) \\
& + \int_\Gamma \sum_{l=1}^{\infty} \frac{k_s^4}{l(l+1)} \sum_{m=-l}^{l} (n_\sigma(x) \times (N_{lm}(x) \times n_\sigma(x))) \, \overline{M_{lm}(y)} \cdot (\operatorname{curl} E(y) \times n_\gamma(y)) d\gamma(y) \\
& + \int_\Gamma \frac{k_p^2}{t} n_\sigma(x) \sum_{l=0}^{\infty} \sum_{m=-l}^{l} j_l(k_p|y|) \overline{Y_l^m(\hat{y})} (i \ k_p \ h_l(k_p|x|) + k_s \ h_l'(k_p|x|)) Y_l^m(\hat{x}) (E(y) \cdot n_\gamma(y)) d\gamma(y).
\end{aligned}
$$

Let p be a given integer and p^* the integer part of $\sqrt{p}$. We denote $(\mathcal{B}_\Gamma)_p$ the truncation of the operator $\mathcal{B}_\Gamma$ of order p. $(\mathcal{B}_\Gamma)_p$ satisfies

$$
\begin{aligned}
& || \ (\mathcal{B}_\Gamma - (\mathcal{B}_\Gamma)_p) \Psi \ ||_{L^2(\Sigma)^3} \\
\leq \quad & \alpha_1 \sum_{l=p^*+1}^{\infty} \frac{k_s^3}{l(l+1)} \sum_{m=-l}^{l} || \ n_\sigma \times N_{lm} \ ||_{L^2(\Sigma)^3} \ || \ n_\gamma \times \operatorname{curl} M_{lm} \ ||_{L^2(\Gamma)^3} \\
& + \alpha_2 \sum_{l=p^*+1}^{\infty} \frac{k_s^3}{l(l+1)} \sum_{m=-l}^{l} || \ n_\sigma \times \operatorname{curl} N_{lm} \ ||_{L^2(\Sigma)^3} \ || \ n_\gamma \times M_{lm} \ ||_{L^2(\Gamma)^3} \\
& + \alpha_3 \sum_{l=p^*+1}^{\infty} \frac{k_s^2}{l(l+1)} \sum_{m=-l}^{l} || \ n_\sigma \times (\operatorname{curl} N_{lm} \times n_\sigma) ||_{L^2(\Sigma)^3} || \ n_\gamma \times \operatorname{curl} M_{lm} ||_{L^2(\Gamma)^3} \\
& + \alpha_4 \sum_{l=p^*+1}^{\infty} \frac{k_s^4}{l(l+1)} \sum_{m=-l}^{l} || \ n_\sigma \times (N_{lm} \times n_\sigma) \ ||_{L^2(\Sigma)^3} \ || \ n_\gamma \times M_{lm} \ ||_{L^2(\Gamma)^3} \\
& + \alpha_5 \sum_{l=p^*+1}^{\infty} \frac{k_p^2}{t} \sum_{m=-l}^{l} || \ (i \ k_p \ h_l(k_p|.|) + k_s \ h_l'(k_p|.|)) Y_l^m(\hat{.}) \ ||_{L^2(\Sigma)^3} || \ j_l(k_p|.|) Y_l^m(\hat{.}) \ ||_{L^2(\Gamma)^3} ,
\end{aligned}
\tag{42}
$$

where the constants α_i for $i = 1, ..., 4$ depend on $||\operatorname{curl} E||_{H^{1/2}(\Gamma)^3}$ and α_5 depends on $||E \cdot n||_{H^{-1/2}(\Gamma)}$.

Thanks to the expression of the quantities involving N_{lm} and M_{lm}, with respect to the Bessel and Hankel functions, the approximation (42) becomes

$$
\begin{aligned}
& || \, (\mathcal{B}_\Gamma - (\mathcal{B}_\Gamma)_p)\Psi \, ||_{L^2(\Sigma)^3} \\
\leq \quad & \alpha_1 \sum_{l=p^*+1}^{\infty} \frac{k_s^3}{l(l+1)} \sum_{m=-l}^{l} \sqrt{l(l+1)} \mid h_l(k_sR) \mid R \, l(l+1) \mid j_l(k_s) + k j_l'(k_s) \mid \\
& + \alpha_2 \sum_{l=p^*+1}^{\infty} \frac{k_s^3}{l(l+1)} \sum_{m=-l}^{l} \sqrt{l(l+1)} \mid h_l(k_sR) + k_sR h_l'(k_sR) \mid l(l+1) \mid j_l(k_s) \mid \\
& + \alpha_3 \sum_{l=p^*+1}^{\infty} \frac{k_s^2}{l(l+1)} \sum_{m=-l}^{l} \sqrt{l(l+1)} \mid h_l(k_sR) + k_sR h_l'(k_sR) \mid l(l+1) \mid j_l(k_s) + k_s j_l'(k_s) \mid \\
& + \alpha_4 \sum_{l=p^*+1}^{\infty} \frac{k_s^4}{l(l+1)} \sum_{m=-l}^{l} \sqrt{l(l+1)} \mid h_l(k_sR) \mid R \, l(l+1) \mid j_l(k_s) \mid \\
& + \alpha_5 \sum_{l=p^*+1}^{\infty} \frac{k_p^2}{t} \sum_{m=-l}^{l} \mid i k_p h_l(k_pR) + k_s h_l'(k_pR) \mid R \mid j_l(k_p) \mid .
\end{aligned}
\tag{43}
$$

By the asymptotic behavior of the spherical Bessel and Hankel functions for large l, we have the following approximation

$$
\begin{aligned}
|| \, (\mathcal{B}_\Gamma - (\mathcal{B}_\Gamma)_p)\Psi \, ||_{L^2(\Sigma)^3} \leq \quad & c_1 \sum_{l=p^*+1}^{\infty} l\sqrt{l(l+1)} \frac{k_s^2}{R^l} + c_2 \sum_{l=p^*+1}^{\infty} \sqrt{l}(l+1)^{\frac{3}{2}} \frac{k_s^2}{R^{l+1}} \\
& + c_3 \sum_{l=p^*+1}^{\infty} (l(l+1))^{\frac{3}{2}} \frac{k_s}{R^{l+1}} + c_4 \sum_{l=p^*+1}^{\infty} \sqrt{l(l+1)} \frac{k_s^3}{R^l} \\
& + c_5 \sum_{l=p^*+1}^{\infty} (l+1) \frac{k_s}{R^{l+1}},
\end{aligned}
$$

where c_i depend on α_i for $i = 1, ..., 5$ and on the constant induced by the asymptotic behavior of special functions. Thus, using the convergence properties of derivatives of geometric series, we obtain the estimation

$$
|| \, (\mathcal{B}_\Gamma - (\mathcal{B}_\Gamma)_p)\Psi \, ||_{L^2(\Sigma)^3} \leq \; \alpha \, \mathrm{e}^{-\tau(p^*+1)} \leq \; \tilde{\alpha} \, \mathrm{e}^{-\tau\sqrt{p}}
$$

where α, $\tilde{\alpha}$ and τ are positive constants and $\alpha \approx \tilde{\alpha}$.

□

Remark 4.3 *If the surface of the scatterer is not spherical, we can consider an intermediate spherical surface $\widetilde{\Gamma}$ between Γ and the artificial boundary Σ. The artificial boundary condition on Σ can be defined by an integral representation expressed with an integral over $\widetilde{\Gamma}$. To this aim, we remark that the previous proof can be extended to the case of a transmission boundary condition on $\widetilde{\Gamma}$.*

Proposition 4.4 *The application of GMRES to Problem (34) has superlinear convergence.*

Proof: Considering γ_p, $p \geq 0$, the singular values of $\mathcal{B}_\Gamma$, denoting by r_m the residual at iteration m and by μ_p, $p \geq 0$, the singular values of $(\mathcal{K})^{-1}$ where

$$
\mathcal{K} = \mathcal{I} + \mathcal{B}_\Gamma \, ,
$$

since $\mathcal{K}$ is a bijective continuous operator with continuous inverse $\mathcal{K}^{-1}$, the singular values μ_p of $\mathcal{K}^{-1}$ are bounded and Theorem 1 of [25] implies

$$|| \, r_m \, ||_{L^2(\Sigma)^3} \leq (\prod_{p=1}^{m} \gamma_p \mu_p) \, || \, \widetilde{\mathcal{F}}_t \, ||_{L^2(\Sigma)^3} \ .$$

Then, by Proposition 4.2

$$\gamma_p \leq \frac{\tilde{\alpha}}{p^\tau} \qquad \forall p \geq 1, \ \tilde{\alpha} \geq 0.$$

Thus,

$$|| \, r_m \, ||_{L^2(\Sigma)^3} \leq \beta \frac{\tilde{\alpha}^m}{m!^\tau},$$

where β is a positive constant which depends on $|| \, \widetilde{\mathcal{F}}_t \, ||_{L^2(\Sigma)^3}$. The approximation of $m!$ by Stirling's formula gives the following expression

$$|| \, r_m \, ||^{\frac{1}{m}}_{L^2(\Sigma)^3} \leq \frac{c}{m^\tau} \quad \forall m \geq 0.$$

Therefore,

$$\lim_{m \to \infty} || \, r_m \, ||^{\frac{1}{m}}_{L^2(\Sigma)^3} = 0 \, .$$

This justifies that we have a superlinear convergence of the GMRES method.

□

5. Numerical results

This section is dedicated to the numerical resolution of Problem (9). To this aim, we use the GMRES preconditioned by the Schwarz preconditioner introduced in previous sections. Considering a finite element discretization $\mathcal{T}_h$ of the domain Ω delimited by Γ and Σ, the Hilbert space $\mathcal{H}_t$ is approximated by V_h, $h > 0$, defined by

$$V_h = \left\{ v_h \in C^0 \left(\bar{\Omega}\right)^3 ; v_{h|_K} \in \mathbb{P}_m \left(K\right)^3 , \forall K \in \mathcal{T}_h \right\},$$

where $\mathbb{P}_m$ is the set of polynomials of degree $\leq m$. If N designates the total number of degrees of freedom, V_h is generated by the vectorial functions $w_j \mathbf{e}_k$, $j = 1, ..., N$ and $k = 1, 2, 3$, where $(\mathbf{e}_i)_{i=1,...,3}$ is the canonical basis of $\mathbb{R}^3$ and $(w_i)_{i=1,...,N}$ is the unidimensional Lagrange finite element basis of order m.

The numerical implementation was done using and developing new integrands in the finite element library MÉLINA++ ([23]). The discretization of Problem (9) is motivated by this consideration. The discrete unknown E_h is decomposed as follows:

$$E_h = \sum_{j=1}^{N} E_j w_j \quad \text{with} \quad E_j = E_j^1 \mathbf{e}_1 + E_j^2 \mathbf{e}_2 + E_j^3 \mathbf{e}_3 \, .$$

Choosing the test functions $E'_h = w_i \mathbf{e}_k$, $k = 1, ..., 3$, $i = 1, ..., N$, the discrete system becomes

$$\forall k \in \{1, ..., 3\}, \ \forall i \in \ \{1, ..., N\}, \qquad \sum_{j=1}^{N} \sum_{l=1}^{3} ((\mathcal{A}_t w_j \mathbf{e}_l, w_i \mathbf{e}_k)_t + (\mathcal{C}_t w_j \mathbf{e}_l, w_i \mathbf{e}_k)_t) E_j^l = (F_t, w_i \mathbf{e}_k)_t \, ,$$

which is equivalent to

$$(A + C)E = F \, ,$$

where A and C are defined blockwise by

$$A = (A_{ij})_{i,j=1,...,N} \quad \text{and} \quad C = (C_{ij})_{i,j=1,...,N} \, ,$$

with, for all $i, j \in \{1, ..., 3\}$, $(A_{ij})_{kl} = (\mathcal{A}_t w_j \mathbf{e}_l, w_i \mathbf{e}_k)_t$ and $(C_{ij})_{kl} = (\mathcal{C}_t w_j \mathbf{e}_l, w_i \mathbf{e}_k)_t$. The matrix C involves the integral operators and the matrix A is related to the differential operators. In order to take

in consideration the essential condition in this use of the library MÉLINA++, we consider a penalization strategy ([2]):

$$\varepsilon_p \, (n_\gamma \times \operatorname{curl} E) + E \times n_\gamma = 0 \;\text{ with }\; \varepsilon_p > 0,$$

such that the matrix A is added to a term A_{ε_p} resulting from this penalization strategy.

We then consider $\widetilde{A} = A + A_{\varepsilon_p}$ as the Schwarz preconditioner, and the system to be solved is

$$(I + \widetilde{A}^{-1}C)E = \widetilde{A}^{-1}F. \tag{44}$$

As a first step of the numerical investigation, we validate the convergence of the preconditioned CEFRI strategy by the consideration of an intermediate problem the solution of which is known:

$$\begin{cases} \operatorname{curl}\operatorname{curl} E - \nabla(\operatorname{div} E) - k_s^2 E = 0 \text{ in } \Omega_e, \\ E \times n_\gamma = \mathcal{G}_1^1(.,x_0) \times n_\gamma, \operatorname{div} E = \operatorname{div} \mathcal{G}_1^1(.,x_0) \text{ on } \Gamma, \\ \lim\limits_{\rho\to\infty} \int_{||x||=\rho} ||\operatorname{curl} E^s \times n_e - ik_s n_e \times (E^s \times n_e)||^2 d\gamma = 0, \\ \lim\limits_{\rho\to\infty} \int_{||x||=\rho} |\operatorname{div} E^s - ik_s E^s \cdot n_e|^2 d\gamma = 0, \end{cases} \tag{45}$$

where $\mathcal{G}_1^1(.,x_0)$, the first component of the vector $\mathcal{G}_1$, is the solution of Problem (45) and x_0 is an artificial source point which belongs to the scatterer and is chosen equal to $(0,0,0.01)$ in this test case. The scatterer is the unit ball and the artificial boundary Σ is the sphere concentric to Γ with radius $R = 1.5$. In this section, the stopping criterion of GMRES corresponds to a residual lower than 10^{-6}.

Table 1

Error on solution and behavior of the residuals $= \dfrac{||(I + \widetilde{A}^{-1}C)E_c - \widetilde{A}^{-1}F||_2}{||\ \widetilde{A}^{-1}F\ ||_2}$, case $k_s = 3, h = 0.3$.

ε_p	$\dfrac{\|\|E_c - E_e\ \|_2}{\|\ E_e\ \|_2}$	$\dfrac{\|\|(\widetilde{A}+C)(E_c-E_e)\|\|_2}{\|\ (\widetilde{A}+C)E_e\|\|_2}$	Residuals	Iterations
10^{-2}	1.35	0.05	4×10^{-7}	48
10^{-3}	1.19	0.01	5×10^{-7}	44
10^{-4}	5.8	0.01	2×10^{-7}	55
10^{-5}	23	0.01	3×10^{-7}	43
10^{-6}	75	0.01	9×10^{-8}	43

Table 1 shows the relative error on the solution of Problem (45) for different choices of the penalization parameter ε_p for a given wavenumber $k_s = 3$ and a given mesh. E_e is the exact solution of (45) and E_c denotes the numerical solution obtained by the resolution of the discrete system obtained by the preconditioned CEFRI approach. When the residual criterion is fixed, $\frac{||(I+\widetilde{A}^{-1}C)E_c-\widetilde{A}^{-1}F||_2}{||\widetilde{A}^{-1}F||_2} \leq 10^{-6}$, the last column shows that the number of iterations is not significantly sensitive to the penalization parameter. The weighted relative error $\frac{||(\widetilde{A}+C)(E_c-E_e)||_2}{||(\widetilde{A}+C)E_e||_2}$ is encouraging but the relative error on the solution, $\frac{||E_c-E_e||_2}{||E_e||_2}$, seems to be extremely deteriorated by the term A_{ε_p} of the preconditioner $\widetilde{A}$. In order to explain this impact of the penalization strategy, we exhibit spectral numerical properties of the preconditioner $\widetilde{A} = A + A_{\varepsilon_p}$. Tables 2, 3 and 4 show the largest-magnitude eigenvalue $\lambda_{\max}$, the smallest-magnitude eigenvalue $\lambda_{\min}$ and the condition number cond_2 of respectively A, A_{ε_p} and $\widetilde{A}$. The tables clearly show the impact of the penalization strategy on the condition number of the preconditioner when ε_p tends to 0. This explains the disturbance observed on the accuracy of the resolution.

Table 2
Extreme eigenvalues of matrix A, case $h = 0.3$, $k_s = 2.1$, $R = 1.5$.

$\lambda_{\max}$	$\lambda_{\min}$	cond_2
14.4865 - $(7.32195 \times 10^{-6})\ i$	0.0859181 - 0.087054 i	118.43854

Table 3
Extreme eigenvalues of matrix A_{ε_p}, case $h = 0.3$, $k_s = 2.1$, $R = 1.5$.

ε_p	$\lambda_{\max}$	$\lambda_{\min}$	cond_2
10^{-2}	8.84872	6.51797×10^{-7}	1.357×10^{7}
10^{-3}	88.4582	7.66253×10^{-7}	1.154×10^{8}
10^{-4}	884.565	-2.04043×10^{-7}	4.335×10^{9}
10^{-5}	8845.66	7.35942×10^{-7}	1.202×10^{10}
10^{-6}	88456.7	9.1692×10^{-7}	9.647×10^{10}

Table 4
Extreme eigenvalues of matrix $\widetilde{A} = A + A_{\varepsilon_p}$, case $h = 0.3$, $k_s = 2.1$, $R = 1.5$.

ε_p	$\lambda_{\max}$	$\lambda_{\min}$	cond_2
10^{-2}	16.2733 - $(4.46251 \times 10^{-6})\ i$	0.111321 + 0.111321 i	103.36
10^{-3}	89.2469 - $(1.60268 \times 10^{-8})\ i$	0.141682 - 0.123085 i	475.52
10^{-4}	885.346 - $(1.3209 \times 10^{-10})\ i$	0.153267 - 0.135483 i	4327.96
10^{-5}	8846.45 - $(1.1022 \times 10^{-12})\ i$	0.154249 - 0.135636 i	43069.01
10^{-6}	88457.5 - $(1.57468 \times 10^{-12})\ i$	0.154346 - 0.135646 i	430489.5

The value of the regularization parameter also impacts the application of the preconditioner $\widetilde{A}$ which is performed by a LU resolution. In table 5, we show the accuracy of the resolution by the LU solver. The error indicated in the second line corresponds to the difference between the initial right hand side and the right hand side recalculated from the obtained solution: LU_error $=|| \widetilde{A}X - b \,||\, / \,|| \, b \, ||$ where X is the solution of the system $\widetilde{A}X = b$ obtained by LU solver, and b is a given right hand side.

Table 5
Error on LU resolution with respect to ε_p; case $h = 0.3, k_s = 2.1$, $R = 1.5$.

ε_p	10^{-2}	10^{-3}	10^{-4}	10^{-5}	10^{-6}	10^{-7}
LU_error	3×10^{-15}	8×10^{-14}	5×10^{-12}	4×10^{-10}	8×10^{-7}	4×10^{-3}

Finally, still for Problem (45), in Fig. 9, we plot the weighted relative error with respect to the average edgelength of the mesh, for different values of ε_p. This result, combined with the prior ones, suggests the choice of $\varepsilon_p = 10^{-4}$ as a good compromise.

As a second step, we apply the preconditioned CEFRI strategy to the initial problem (2). Indeed, we solve Equation (30), the discretization of which is given by Equation (44). We consider the case of an incident plane wave with the direction (0, 0, 1) and the polarization (1, 0, 0). We choose $\nu_1 = \nu_2 = -ik_s$, the regularization parameter $t = 1$ and the penalty parameter $\varepsilon_p = 10^{-4}$. Moreover, we consider meshes such that the average edgelength and the distance between the boundaries remains constant with respect to the wavelength. In Figure 10, we show the residuals of GMRES at every restart. The study is done for the wavenumbers $k_s = 1.25$, $k_s = 2.5$ and $k_s = 5$. Through these test cases, we conclude that the asymptotic behavior of GMRES validates the theoretical study done in previous sections.

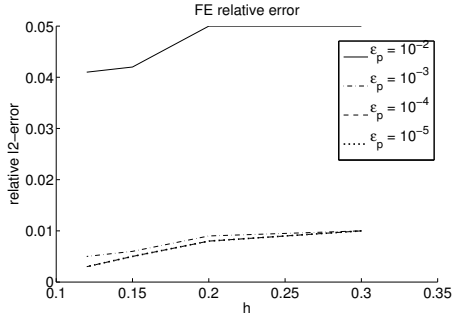

Figure 9. Relative l^2-error on solution with respect to discretization, case $k_s = 3$

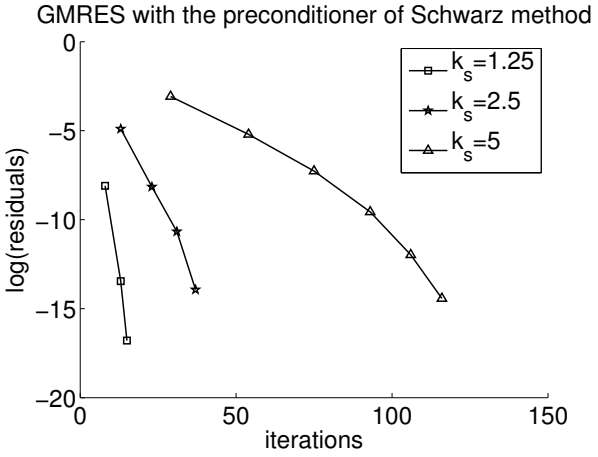

Figure 10. Behavior of the residuals of GMRES preconditioned by A, case hk_s fixed, $\varepsilon_p = 10^{-4}$.

6. Conclusion

This work firstly contributed to a theoretical analysis and justification of an algorithm for the resolution of the 3D exterior Maxwell problem using a combination of finite elements and integral representation. This algorithm introduced by Jin and Liu ([21]) was interpreted as a Schwarz method with total overlap. In such a way, we analytically characterized the convergence of the algorithm depending on the distance between the surface of the obstacle and the artificial surface. The theoretical result reveals the finite element term of the Schwarz method as a preconditioner for Krylov solvers. A significant result derived in this paper is the superlinear convergence of the GMRES algorithm when it is preconditioned with the so called Schwarz preconditioner in the case of the scattering of a time-harmonic electromagnetic wave by a perfect conductor: the superlinear convergence were first analytically justified in the spherical configuration; then, numerical tests confirmed this behavior using and contributing to the development of the finite element library MÉLINA++ ([23]).

Such results justify further investigations in the consideration of the combination of finite elements and integral representation. Next important aspects for the numerical resolution will be the use of edge elements to avoid the regularization technique and the use of fast methods such as the fast multipole method. A significant perspective would be the extension of the study to other boundary conditions like

transmission condition or other geometrical configurations such as geometries with singularities ([12]).

References

[1] X. Antoine, H. Barucq, A. Bendali, Bayliss-Turkel-like radiation condition on surfaces of arbitrary shape, J. Math. Anal. Appl., vol. 229, pp 184-211, 1999.

[2] J. W. Barrett, C. M. Elliott, Finite Element Approximation of the Dirichlet Problem Using the Boundary Penalty Method, Numer. Math., vol. 49, pp 343-366, 1986.

[3] N. Bartoli, F. Collino, Etude bidimensionnelle de la condition absorbante adaptative proposée par Liu et Jin pour la résolution des problèmes de diffraction, CERFACS REPORT TR/EMC/04/34, 56 pages, 2004.

[4] A. Bayliss, M. Gunzburger, E. Turkel, Boundary conditions for the numerical solution of elliptic equations in exterior regions, SIAM J. Appl. Math., vol. 42, no. 2, pp 430-451, 1982.

[5] F. Ben Belgacem, M. Fournié, N. Gmati, F. Jelassi, On the Schwarz algorithms for the elliptic exterior boundary value problems, M2AN Math. Model. Numer. Anal., vol. 39, No. 4, pp 693-714, 2005.

[6] F. Ben Belgacem, N. Gmati, F. Jelassi, Convergence bounds of GMRES with Schwarz' preconditioner for the scattering problem. Int. J. Numer. Meth. Engng., 80:191-209, 2009.

[7] A. Bendali, L. Halpern, Approximation par troncature de domaine de la solution du problème aux limites extérieur pour le système de Maxwell en régime sinusoïdal, C. R. Acad. Sci. Paris Ser. I Math., vol. 294, pp 557-560, 1982.

[8] J-P. Berenger, A perfectly matched layer for the absorption of electromagnetic waves, J. Comput. Phys., vol. 114, pp 185-200, 1994.

[9] D. Colton, R. Kress, Inverse Acoustic and Electromagnetic Scattering Theory, 2nd Edition, Springer-Verlag, Berlin, 1998.

[10] M. Costabel, A coercive bilinear form for Maxwell's equations, J. Math. Anal. Appl., vol. 157, pp 527-541, 1991.

[11] M. Costabel, M. Dauge, Maxwell and Lamé eigenvalues on polyhedra, Math. Methods Appl. Sci., vol. 22, pp 243-258, 1999.

[12] M. Costabel, M. Dauge, Weighted regularization of Maxwell equations in polyhedral domains. A rehabilitation of nodal finite elements, Numer. Math., vol. 93, pp 239-277, 2002.

[13] M. Costabel, M. Dauge, D. Martin, G. Vial, Weighted regularization of Maxwell equations: computations in curvilinear polygons, Numerical mathematics and advanced applications, Springer Italia, Milan, pp 273-280, 2003.

[14] M. Costabel, M. Dauge, S. Nicaise, Singularities of Maxwell interface problems, M2AN Math. Model. Numer. Anal., vol. 33, pp 627-649, 1999.

[15] E. Darrigrand, P. Monk, Coupling of the Ultra-Weak Variational Formulation and an Integral Representation using a Fast Multipole Method in Electromagnetism. J. Comput. Appl. Math., 204 (2), pp 400-407, 2007.

[16] R. Djellouli, C. Farhat, A. Macedo, R. Tezaur, Finite element solution of two-dimensional acoustic scattering problems using arbitrarily shaped convex artificial boundaries, J. Comput. Acoust., vol. 8, pp 81-99, 2000.

[17] V. Girault, P.A. Raviart, Finite element methods for Navier-Stokes equations, Springer Series in Computational Mathematics, vol. 5, Theory and algorithms, Springer-Verlag, Berlin, 1986.

[18] N. Gmati, B. Philippe, Comments on the GMRES Convergence for preconditioned systems, Large-Scale Scientific Computing, Lecture Notes in Comput. Sci., Springer, pp. 40-51, 2008.

[19] C. Hazard, M. Lenoir, On the solution of time-harmonic scattering problems for Maxwell's equations, SIAM J. Math. Anal., vol. 27, no. 6, pp 1597-1630, Nov. 1996.

[20] A. Jami, M. Lenoir, Formulation variationnelle pour le couplage entre une méthode d'éléments finis et une représentation intégrale, C. R. Acad. Sci. Paris Sér. A-B, vol. 285, no. 4, pp A269-A272, 1977.

[21] J. Liu, J-M. Jin, A novel hybridization of higher order finite element and boundary integral methods for electromagnetic scattering and radiation Problems, IEEE Trans. Antennas and Propagation, vol. 49, No. 12, pp 1794-1806, Dec. 2001.

[22] J. Liu, J-M. Jin, A Highly Effective Preconditioner for Solving the Finite Element-Boundary Integral Matrix Equation of 3-D Scattering. IEEE Trans. Antennas and Propagation, vol. 50, no. 9, pp 1212-1221, 2002.

[23] D. Martin, E. Darrigrand, and Y. Lafranche, http://anum-maths.univ-rennes1.fr/melina/melina++_distrib/ (MÉLINA++ documentation), Université Rennes 1, last update: apr 2015.

[24] P. Monk, Finite element methods for Maxwell's equations, Numerical Mathematics and Scientific Computation, Oxford University Press, New York, 2003.

[25] I. Moret, A note on the superlinear convergence of GMRES, SIAM J. Numer. Anal., vol. 34, pp 513-516, 1997.

[26] P. M. Morse, H. Feshbach. Methods of theoretical physics, Part II, McGraw-Hill, New York, USA, 1953.

[27] J-C. Nédélec, Acoustic and electromagnetic equations – Integral representations for harmonic problems, Applied Mathematical Sciences, Springer-Verlag, New York, vol. 144, 2001.

[28] R. Tezaur, A. Macedo, C. Farhat, R. Djellouli, Three-dimensional finite element calculations in acoustic scattering using arbitrary shaped convex artificial boundaries, Int. J. Numer. Meth. Engng., vol. 53, pp 1461-1476, 2002.

[29] H. Weyl, Das asymptotische Verteilungsgesetz der Eigenwerte linearer partieller Differentialgleichungen (mit einer Anwendung auf die Theorie der Hohlraumstrahlung) (German). Math. Ann., vol. 71, pp 441-479, 1912.

[30] N. Zerbib, F. Collino, F. Millot, Etude tridimensionnelle de la condition absorbante adaptative proposée par Liu et Jin pour la résolution des problèmes de diffraction, CERFACS REPORT TR/EMC/05/81, 30 pages, 2005.